# Evaluation of Cyclic Amides as Activating Groups in N–C Bond Cross-Coupling: Discovery of N-Acyl-δ-Valerolactams as Effective Twisted Amide Precursors for Cross-Coupling Reactions

*Md. Mahbubur Rahman,[†] Daniel J. Pyle,[†] Elwira Bisz,[‡] Błażej Dziuk,[‡,||] Krzysztof Ejsmont,[‡] Roger Lalancette,[†] Qi Wang,[¶] Hao Chen,[¶] Roman Szostak,[§] and Michal Szostak*[,†]*

[†]Department of Chemistry, Rutgers University, 73 Warren Street, Newark, New Jersey 07102, United States

[‡]Department of Chemistry, Opole University, 48 Oleska Street, Opole 45-052, Poland

[||]Department of Chemistry, Wroclaw University of Science and Technology, Norwida 4/6 14, Wroclaw 50-373, Poland

[¶]Department of Chemistry & Environmental Science, New Jersey Institute of Technology, Newark, NJ 07102, USA

[§]Department of Chemistry, Wroclaw University, F. Joliot-Curie 14, Wroclaw 50-383, Poland

**Corresponding author**

michal.szostak@rutgers.edu

**TOC Graphic**

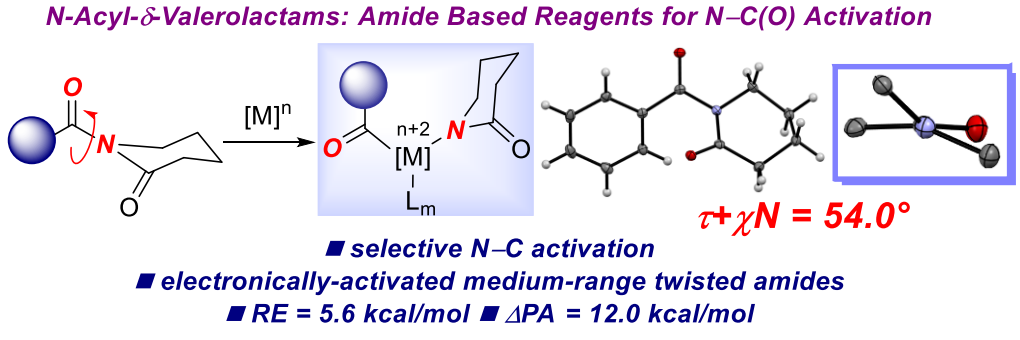

The development of efficient methods to facilitate N–C(O) bond activation in amides is an important objective in organic synthesis that permits for manipulation of the traditionally unreactive amide bonds. Herein, we report a comparative evaluation of a series of cyclic amides as activating groups in amide N–C(O) bond cross-coupling. Evaluation of N-acyl-imides, N-acyl-lactams, and N-acyl-oxazolidinones bearing five- and six-membered rings using Pd(II)–NHC and Pd–phosphine systems reveals the relative reactivity order of N–activating groups in Suzuki–Miyaura cross-coupling. The reactivity of activated phenolic esters and thioesters is evaluated for comparison in O–C(O) and S–C(O) cross-coupling under the same reaction conditions. Most notably, the study reveals N-acyl-δ-valerolactams as a highly effective class of mono-N-acyl-activated amide precursors in cross-coupling. The x-ray structure of the model N-acyl-δ-valerolactam is characterized by the additive Winkler-Dunitz distortion parameter $\Sigma(\tau+\chi_N)$ of 54.0°, placing this amide in a medium distortion range of twisted amides. Computational studies provide insight into structural and energetic parameters of the amide bond, including amidic resonance, N-/O-protonation aptitude and rotational barrier around the N–C(O) axis. This class of N-acyl-lactams will be a valuable addition to the growing portfolio of amide electrophiles for cross-coupling reactions by acyl-metal intermediates.

## 1. Introduction

Amides represent one of the most fundamental functional groups in organic chemistry and biology.[1–3] Although typical amides are planar and unreactive as a consequence of $n_N \rightarrow \pi^*_{C=O}$ resonance rendering the N–C(O) bond approximately 40% double in character, recent years have witnessed significant advances in the development of an array of selective methods for N–C(O) bond activation by transition metal catalysis enabled by resonance tuning of the amide bond (Figure 1A).[4] In this respect, early studies by Garg, Zou and our group established N-acyl-Boc-carbamates, N-acyl-Ts-sulfonamides and N-acyl-glutarimides as effective cross-coupling partners by N–C(O) bond activation.[5–7] Although a number of another amide precursors have been developed, N-acyl-glutarimides represent the most reactive amide bond precursors for cross-coupling reactions developed to date (Figure 1B).[8–10]

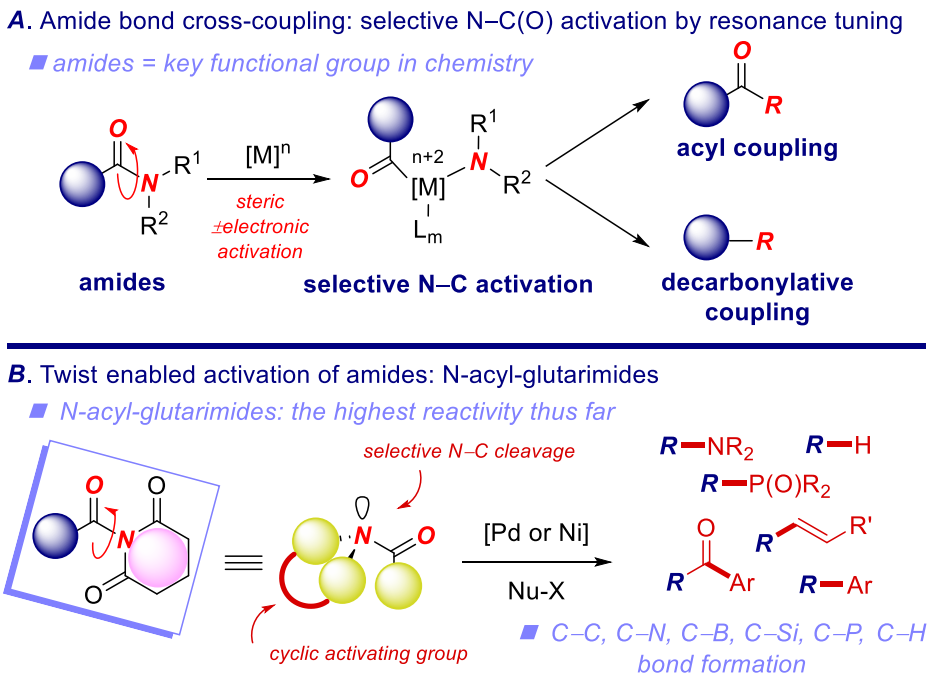


**Figure 1.** (a) Amide bond activation. (b) N-Acyl-glutarimides: twist enabled activation of amide bonds.

Principally, the high reactivity of the amide bond in N-acyl-glutarimides stems from the combination of steric and electronic activation of the amide bond, which results in electronically-disconnected (RE, resonance energy, 0.5-2.4 kcal/mol), twisted amides (twist angle, $\tau$ = 89.1°).[11,12] Considering that N-

acyl-glutarimides constitute privileged amide derivatives that have enabled a range of previously unattainable cross-coupling reactions of amide bonds by C–C, C–N, C–B, C–Si, C–P, C–H bond forming events,[4–10] while at the same time constitute bench- and air-stable stable amide based reagents despite considerable amide bond twist,[13–16] expanding the portfolio of cyclic amides related to glutarimides as activating groups for N–C(O) bond cross-coupling is especially attractive.

In continuation of our studies on amide N–C(O) bond activation[4a,b,7] and geometric and electronic properties of non-planar amide bonds,[11,12] herein we report a comparative evaluation of a series of cyclic amides as activating groups in amide bond N–C(O) cross-coupling. The study outlines the relative reactivity order of a series of N-acyl-imides, N-acyl-lactams, and N-acyl-oxazolidinones embedded in five- and six-membered rings as well as activated phenolic esters and thioesters by N–C(O), O–C(O) and S–C(O) cleavage using Pd(II)–NHC and Pd–phosphine systems. Most importantly, the study reveals N-acyl-δ-valerolactams as a highly effective class of mono-N-acyl-activated amide precursors in cross-coupling. Reactivity, structural and computational studies have been employed to gain insight into the high propensity of the amide bond in N-acyl-δ-valerolactams to undergo N–C(O) bond cross-coupling. Collectively, this class of mono-N-acyl-lactams will be a valuable addition to the growing portfolio of amide bond electrophiles for cross-coupling reactions.

In general, the development of amide bond cross-coupling reactions relies on the availability of new amide bond derivatives for cross-coupling.[4–10] This is clearly demonstrated by N-acyl-glutarimides, introduced by our group in 2015.[7,8] Now, N-acyl-glutarimides are the reagents of choice for the development of acyl and decarbonylative cross-coupling reactions of amides that have enabled the discovery of more than 10 distinct and previously unknown methods of reactivity of the amide bond. Furthermore, novel amide bond derivatives with distinct steric and electronic features enable reaction fine-tuning due to changes in resonance, sterics around the amide bond and leaving group capacity.[4–12] In this context, N-acyl-δ-valerolactams represent novel mono-acyl-activated equivalents of N-acyl-glutarimides that differ in amidic resonance, sterics around the amide bond and p$K_a$ of the leaving group. The fact that there is no other amide derivative available that covers similar range of steric

distortion and electronic delocalization[4–12] means that these reagents should be routinely included in the development and optimization of amide bond cross-coupling reactions.

## 2. Results and Discussion

Considering that the high reactivity of N-acyl-glutarimides results from the presence of the doubly electronically-activated N-acyl glutarimide ring that additionally sterically-enforces the acyl amide bond from planarity by avoiding syn-pentane-type interactions between the exo- and endo-cyclic carbonyl groups,[11,12] we selected a number of cyclic imide, lactam and oxazolidinone derivatives as activating groups for the study. The structures of the selected compounds are presented in Figure 2. In addition, we selected activated phenolic esters[17] and thioesters[18] to evaluate the capacity of X–C(O) bond in cross-coupling under the same reaction conditions.

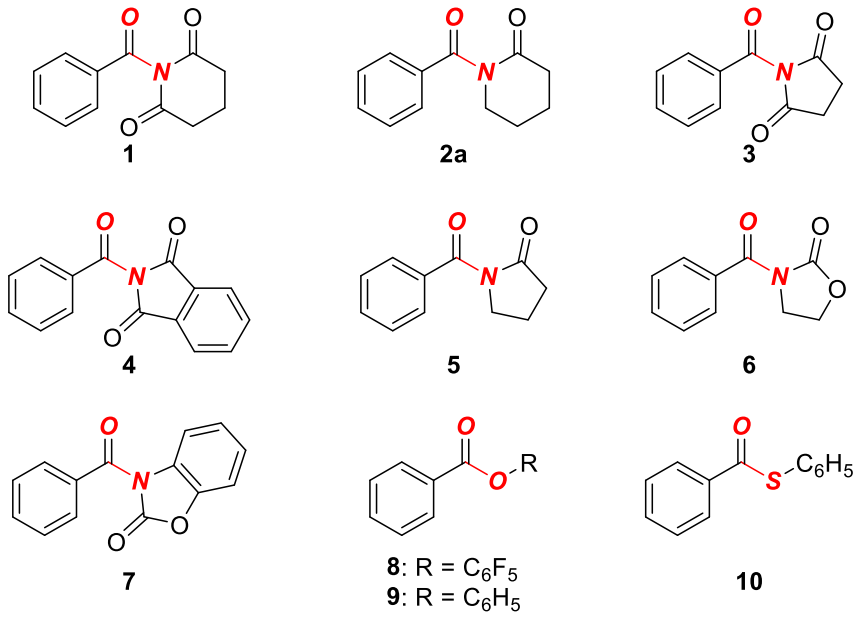


**Figure 2.** Structures of amides and derivatives used in the present study.

The selected compounds include the model N-benzoylglutarimide (**1**), N-benzoyl-δ-valerolactam (**2a**), N-benzoylsuccinimde (**3**), N-benzoylphthalimide (**4**), N-benzoyl-2-pyrrolidinone (**5**), N-benzoyl-2-oxazolidinone (**6**), N-benzoyl-2-benzoxazolinone (**7**) as amide-based derivatives as well as pentafluorophenyl benzoate (**8**), phenyl benzoate (**9**) and S-phenyl benzothioate (**10**) as representative ester and thioester-based acyl electrophiles. In general, the selection was guided by evaluation of (**1**)

mono- vs. double-electronic activation of the cyclic ring (**1** vs. **2a**, **3** vs. **5**); (2) 5- vs. 6-membered ring size of the activating ring (**1** vs. **3**, **2a** vs. **5**); (3) effect of heteroatoms in the ring (**3** vs. **6**); (4) effect of aromatic substitution of the ring (**3** vs. **4**, **6** vs. **7**); and (5) effect of N–C(O) vs. O–C(O) and S–C(O) activation (**1-7** vs. **8-10**). The Suzuki–Miyaura cross-coupling was selected as a test reaction due to the robustness of this coupling and the fact that several complementary catalytic systems have been developed for this reaction using amide-based electrophiles.[4a,b] Due to the high efficiency in the cross-coupling, we selected Pd(II)–NHC systems, such as allyl-based [Pd(IPr)(cin)Cl][19] and heterocycle-based Pd–PEPPSI–IPr[20] as well as $[Pd(PCy_3)_2Cl_2]$[21] as a well-defined Pd(II)–phosphine system and the in situ formed $Pd(OAc)_2/PCy_3$ system. It should be noted that in general Pd–NHC catalysts outperform Pd–phosphines in amide bond acyl cross-coupling.[4a,b] Furthermore, well-defined Pd(II)–phosphines are preferred over in situ formed Pd/phosphines,[21,22] while IPr and $PCy_3$ have been generally established as privileged NHC and phosphine ligands respectively in Pd-catalyzed amide Suzuki–Miyaura cross-coupling.[4a,b,6,7] The results of the comparative study are presented in Table 1.

**Table 1. Effect of Activating Group on Suzuki–Miyaura Cross-Coupling by N–C Bond Cleavage**[a]

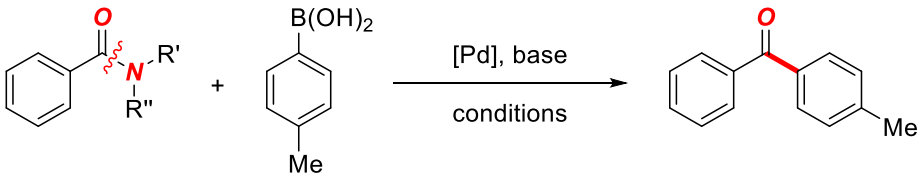


| entry | amide | A | B | C | D |
|---|---|---|---|---|---|
| 1 | 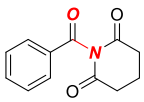 | >98 | >98 | >98 | >98 |
| 2 | 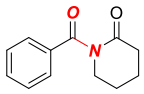 | 92 | 91 | 85 | 73 |
| 3 | 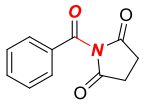 | 66 | 66 | 71 | 85 |
| 4 | 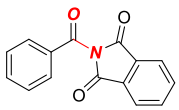 | 44 | 47 | 35 | 32 |
| 5 | 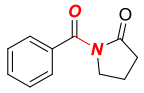 | 54 | 47 | 15 | 12 |

| | | | | | |
|---|---|---|---|---|---|
| 6 | 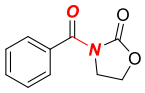 | 66 | 70 | 18 | 18 |
| 7 | 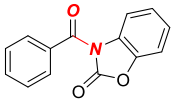 | 24 | 26 | 42 | 35 |
| entry | ester | A | B | C | D |
| 8 | 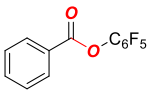 | 62 | 71 | 85 | 90 |
| 9 | 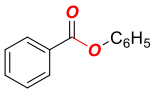 | 51 | 49 | 18 | 17 |
| 10 | 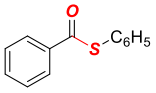 | <5 | <5 | <5 | <5 |

[a]Conditions: amide/ester (1.0 equiv), Ar-B(OH)$_2$ (2.0 equiv), [Pd] (x mol%), base (y equiv), THF (0.25 M), *T*, 15 h. Conditions A: [Pd(IPr)(cin)Cl] (1.0 mol%), $K_2CO_3$ (3.0 equiv), 60 °C. Conditions B: [Pd–PEPPSI–IPr] (1.0 mol%), $K_2CO_3$ (3.0 equiv), 60 °C. Conditions C: [Pd($PCy_3$)$_2$$Cl_2$] (3.0 mol%), $Na_2CO_3$ (2.5 equiv), 120 °C. Conditions D: Pd(OAc)$_2$ (3.0 mol%), $PCy_3HBF_4$ (12 mol%), $Na_2CO_3$ (2.5 equiv), 120 °C. All results are average of at least three independent runs.

As expected, N-acyl-glutarimide (**1**) showed excellent performance under all four conditions (>98% yield, Table 1, entry 1). Unexpectedly, mono-activated N-acyl-δ-valerolactam (**2a**) showed excellent conversion under Pd–NHC conditions (91-92%), while good yields were observed using Pd–$Cy_3$ systems (73-85%) (Table 1, entry 2). *These results suggest that double-activation of amide bond by two exocyclic carbonyl groups is not required for the efficient coupling.* Next, N-acyl-succinimide (**3**) showed considerably lower reactivity using Pd–NHCs (66%), while Pd–$PCy_3$ systems were slightly more effective in this case (71-85%, Table 1, entry 3). Furthermore, conjugation with the fused-aromatic ring in N-acyl-phthalimide (**4**) significantly reduced the reactivity (44-47%, Pd–IPr; 32-35%, Pd–$PCy_3$) (Table 1, entry 4). Interestingly, only a minor decrease in reactivity was observed in the five-membered mono-activated N-benzoyl-2-pyrrolidinone (**5**) using Pd–NHC systems (47-54%), while Pd–phosphine systems were less effective in this case (12-15%) (Table 1, entry 5). An even enhanced effect was found using N-acyl-2-oxazolidinone (**6**), which resulted in 66-70% yields using Pd–NHCs and lower yields using Pd–phosphine systems (18%) (Table 1, entry 2). The effects observed in mono-activated five-membered derivatives (5-6 vs. 3) parallel the reactivity observed in mono-activated six-membered ring (**1** vs. **2a**) using Pd(II)–NHC systems, while six-membered rings are generally more reactive as the

activating group due to lower steric hindrance for oxidative addition. Finally, conjugation with the aromatic ring in N-benzoyl-2-benzoxazolinone (**7**) decreased the reactivity (44-47%, Pd–NHCs; 32-35%, Pd–phosphines) (Table 1, entry 7). This effect is analogous to that observed in succinimide vs. phthalimide derivatives (**3** vs. **4**, **6** vs. **7**) and arises from π-conjugation of the aromatic ring with the exocyclic carbonyl group. To gain further insight into the effect of acyl bond that undergoes cross-coupling, we also evaluated the reactivity of pentafluorophenyl benzoate (**8**), phenyl benzoate (**9**) and S-phenyl benzothioate (**10**) as model ester and thioester substrates for the coupling (Table 1, entries 8-10). Interestingly, pentafluorophenyl benzoate (**8**) showed excellent reactivity using Pd–$PCy_3$ (85-90%) and slightly lower using Pd–NHCs (62-71%) (Table 1, entry 8), while less activated phenyl benzoate was moderately reactive using Pd–NHCs (49-51%) and much less reactive with Pd–$Cy_3$ (17-18%) (Table 1, entry 9). Finally, S-phenyl benzothioate (**10**) was found to be completely unreactive under all conditions tested (<5% conversion, Table 1, entry 10). These results indicate that N–C(O) bond activation in the tested substrates is generally more effective than in O–C(O) and S–C(O) electrophiles. The general reactivity order of amide derivatives can be summarized as follows: N-acyl-glutarimide (**1**) > N-acyl-δ-valerolactam (**2a**) > N-acyl-succinimde (**3**) ≈ pentafluorophenyl benzoate (**8**) > N-acyl-2-oxazolidinone (**6**) > N-acyl-phthalimide (**4**) > N-acyl-2-pyrrolidinone (**5**) > N-acyl-2-benzoxazolinone (**7**) ≈ phenyl benzoate (**9**) > S-phenyl benzothioate (**10**). It is interesting to note that phosphine-type ligands show a different tendency in the coupling from those with NHC ligands. For the NHC system: **1** > **2a** > **3** ≈ **8** > **6** > **4** > **5** > **7** ≈ **9** > **10**; for the phosphine system: **1** > **8** ≈ **2a** ≈ **3** > **7** > **4** > **6** ≈ **9** > **5** > **10**. In general, there are two major considerations, namely stability of the amide precursor to cross-coupling and reactivity of the catalyst system, with NHC being stronger σ-donors.[19,20] In general, less stable amide precursors give inferior results using Pd–phosphines due to side reactions, while stronger σ-donation of Pd–NHCs suggests transmetallation as the rate determining step vs. oxidative addition.[19b]

An interesting finding is that removal of the doubly-activating group to yield mono-activated N-acyl-δ-valerolactam affords high reactivity in amide bond cross-coupling. Furthermore, all amide-based substrates examined showed reactivity across Pd–NHC and Pd–phosphine systems, and while in some

cases the reactivity was low, it is worth noting that prior to 2015 this N–C(O) manifold had been considered beyond the scope of transition-metal-catalyzed cross-coupling reactions.[4–7]

Having identified N-acyl-δ-valerolactams as highly effective amide based cross-coupling reagents, we next explored the scope of these reagents in acyl Suzuki–Miyaura cross-coupling (Schemes 1-2). For the study, we selected allyl-based Pd(II)–NHC precatalyst [Pd(IPr)(cin)Cl] developed by Nolan and co-workers.[4a,19] As shown, the evaluation of the cross-coupling of N-acyl-δ-valerolactams revealed that these reagents show broad scope in the cross-coupling (Scheme 1). As such, electronically-neutral (**12a**), electron-rich (**12b-c**), and electron-deficient (**12d-e**) N-benzoyl-δ-valerolactams coupled in high yields. Furthermore, sterically-hindered (**12f**), biaryl (**12g**) and heterocyclic (**12h**) N-benzoyl-δ-valerolactams are well compatible with the coupling. Of note is the full selectivity for the amide bond coupling in the presence of alkyl ester moiety (**12e**). Furthermore, in all reactions full selectivity for the cleavage of the exocyclic N–C(O) bond was observed (vs. endocyclic N–C(O) bond). The scope of boronic acids is similarly broad and includes electron-neutral (**12i**), electron-rich (**12j**), electron-deficient (**12k-m**), sterically-hindered (**12n-o**), polyaromatic (**12p-q**) and heterocyclic (**12r**) boronic acids (Scheme 2). The distortion of the amide bond is impacted by the steric effect from the substituent on the exocyclic carbonyl.[11–13] Interestingly, amides on five-membered heterocycles, such as furamide derivative (**2h**), show similar distortion of the amide bond to benzamides.[11c,d] Important is full selectivity for the cross-coupling of amide N–C(O) bond in the presence of carbonyl groups (**12l-m**) and chemoselectivity for the cross-coupling of the exo- vs. endo-cyclic N–C(O) bond. Alkyl nucleophiles are not suitable coupling partners in the reaction. The development of Suzuki cross-coupling of amides with alkyl boronic acids is one of the major challenges in amide bond cross-coupling.[4–10] Preliminary studies using Cy–C(O)-δ-valerolactam (Cy = cyclohexyl) as a representative alkyloyl amide gave the product in 32% yield. The use of strongly electron-withdrawing groups, such as 4-CN-$C_6H_4$-$B(OH)_2$ and 4-$NO_2$-$C_6H_4$-$B(OH)_2$ gave the coupling product in modest yields, 29% and 12%. In general, amide bond distortion in alkyloyl derivatives is influenced by the steric effect of the α-carbon substituent with aryl substrates close to secondary alkyl in terms of sterics, while electronically, aryl substituents are

more activated than their corresponding alkyl conterparts.[11a,b] As an important consideration, we have not observed any decomposition of N-acyl-δ-lactams when storing on bench-top over 12 months. In general, the reactivity in amide bond cross-coupling is a balance between the amide bond stability and destabilization onto the adjacent C=O or related groups. In general, single activating exocyclic group provides optimum balance between stability and activation.[4–10]

**Scheme 1. Suzuki–Miyaura Coupling of N-Benzoyl-δ-Valerolactams by N–C(O) Bond Cleavage**[a]

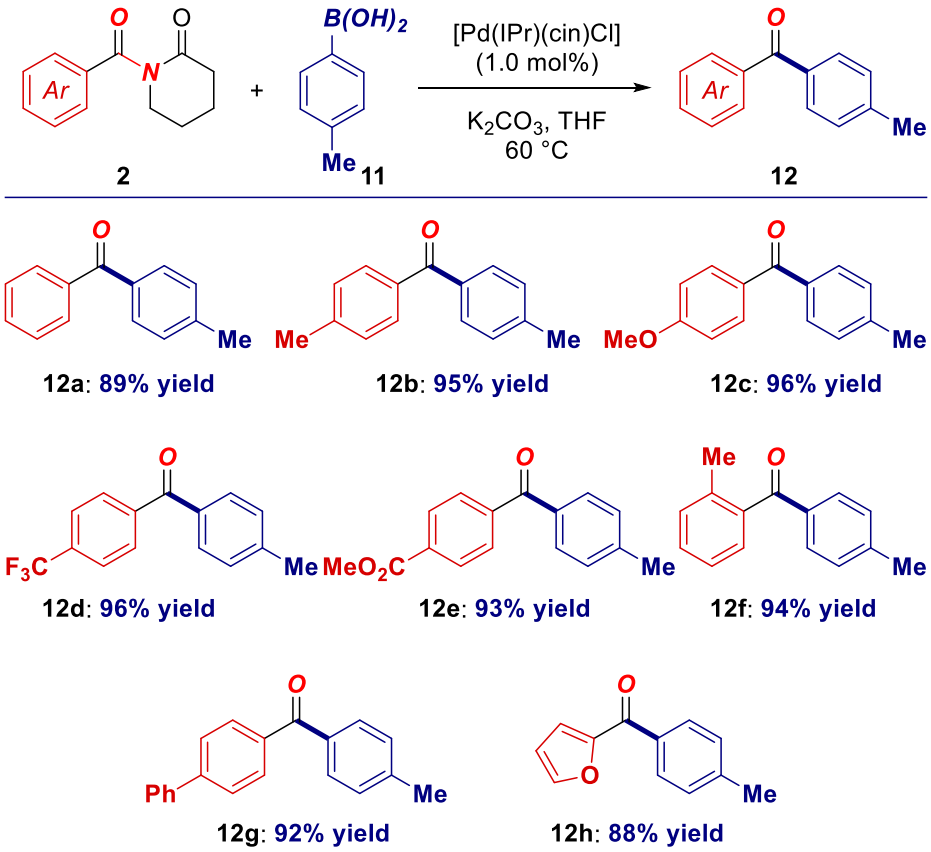


[a]Conditions: amide (1.0 equiv), Ar-B(OH)$_2$ (2.0 equiv), [Pd] (1.0 mol%), $K_2CO_3$ (3.0 equiv), THF (0.25 M), 60 °C, 15 h.

In consideration of the high reactivity of N-acyl-δ-valerolactams, we conducted intermolecular competition experiments to gain insight into the selectivity of the cross-coupling (Schemes 3-4). Thus, intermolecular competition experiments with differently substituted amides revealed that electron-deficient amides are inherently more reactive (4-$CF_3$:4-MeO = 68:32) (Scheme 3A), while ortho-unsubstituted amides are more reactive than sterically-hindered counterparts (H:2-Me = 93:7) (Scheme

3B). Furthermore, competition experiments revealed that electron-rich boronic acids cross-coupling preferentially (4-MeO:4-$CF_3$ = 76:24) (Scheme 4A), while sterically-hindered boronic acids are more reactive (2-Me:4-Me = 66:34) (Scheme 4B). Overall, these findings suggest that oxidative addition may be the rate limiting step in the reaction, however this is a complex scenario including both transmetallation and reductive elimination.[19b,20] In general, the mechanism of amide bond cross-coupling using Pd(II)–NHC systems has been studied by DFT methods, where it was found that depending of the type of precatalyst, the catalyst activation or transmetallation might be kinetically relevant steps in the coupling.[19b]

**Scheme 2. Suzuki–Miyaura Coupling of N-Benzoyl-δ-Valerolactams by N–C(O) Bond Cleavage**[a]

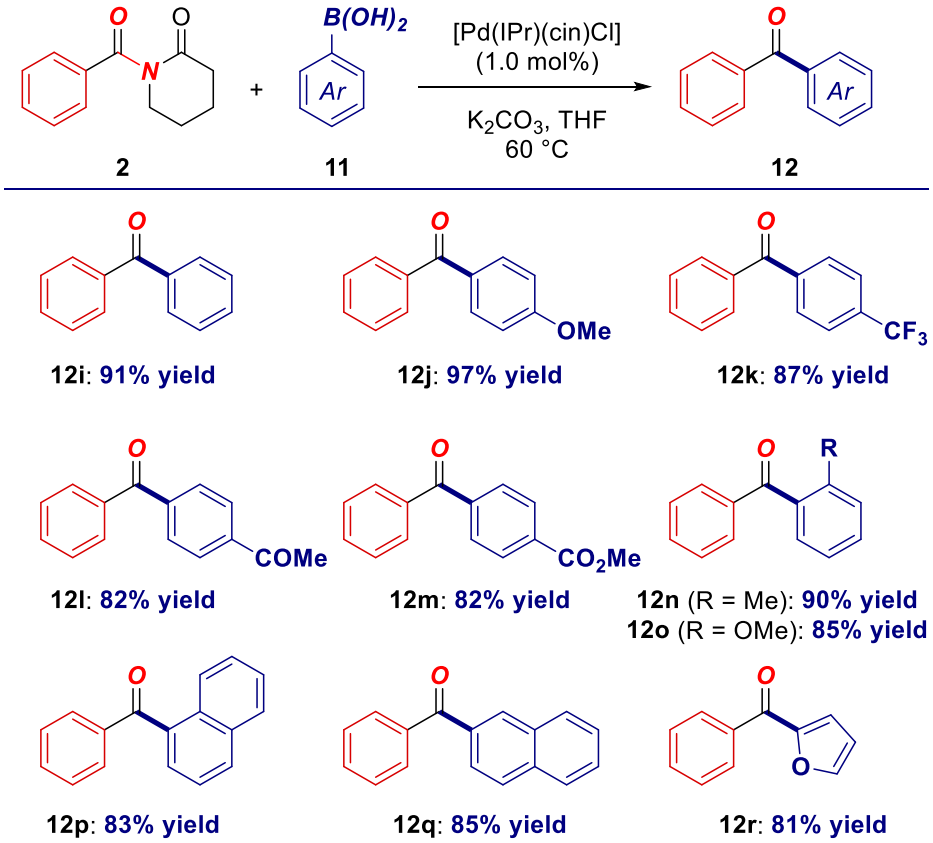


[a]Conditions: amide (1.0 equiv), Ar-$B(OH)_2$ (2.0 equiv), [Pd] (1.0 mol%), $K_2CO_3$ (3.0 equiv), THF (0.25 M), 60 °C, 15 h.

**Scheme 3. Competition Experiments Amides**

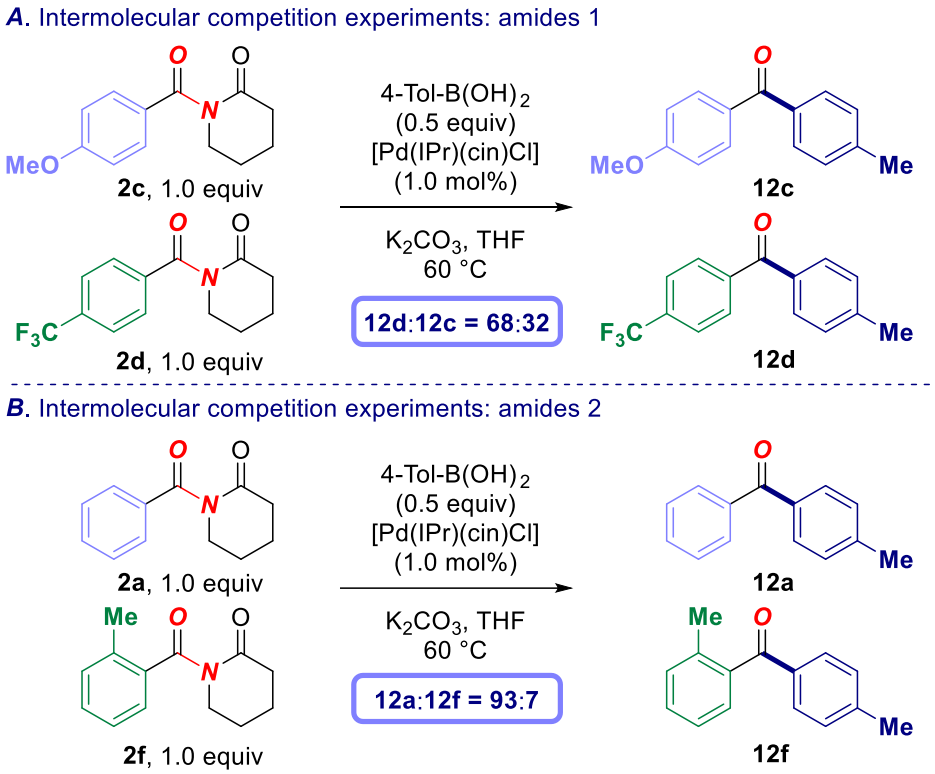


**Scheme 4. Competition Experiments Boronic Acids**

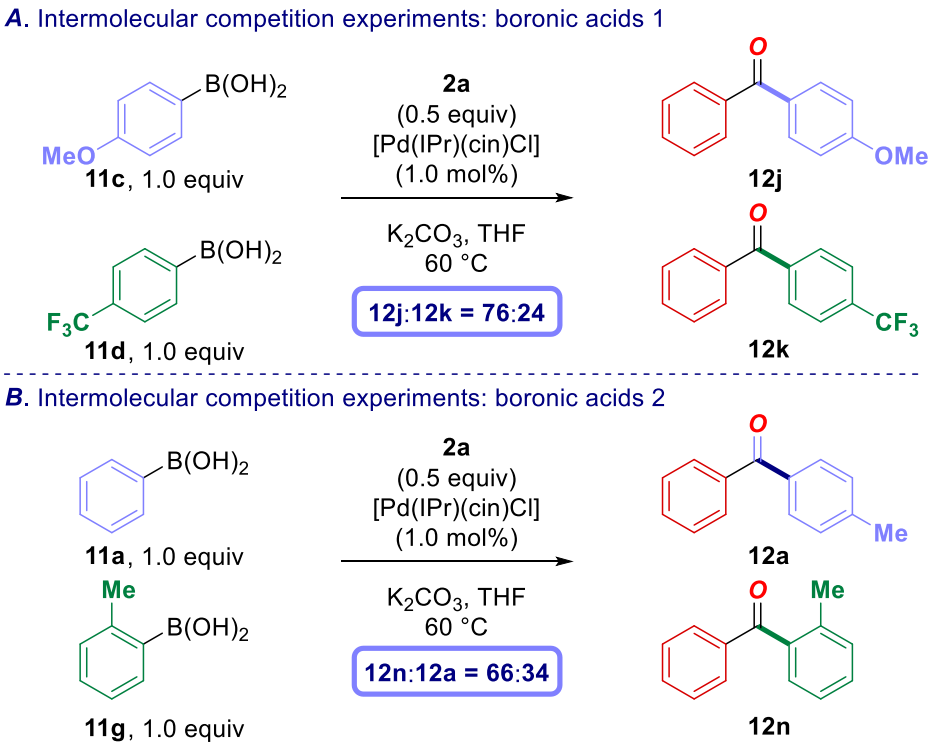


**Crystallographic studies.** To gain insight into the structural properties of the amide bond in N-acyl-δ-valerolactams, the x-ray structure of **2a** was determined (Figure 3, CCDC = 2082397). X-ray quality crystals were obtained by slow evaporation method from $CH_2Cl_2$. Interestingly, the acyclic amide bond

shows moderate distortion from planarity ($\tau$ = 33.2°, $\chi_N$ = 20.8°, $\chi_C$ = 7.0°),[11–16] which corresponds to additive Winkler-Dunitz distortion parameter $\Sigma(\tau+\chi_N)$ of 54.0°,[14d] placing this amide in a medium distortion range of twisted amides. The Winkler-Dunitz parameters ($\tau$, $\chi_N$, $\chi_C$) were calculated according to ref. 14e. Twist ($\tau$) quantifies the magnitude of rotation around the N–C(O) bond; pyramidalization at nitrogen ($\chi_N$) and at carbon ($\chi_C$) describe pyramidalization at nitrogen and pyramidalization at carbon, respectively. The exocyclic N–C(O) and C=O bond lengths are 1.408 Å and 1.216 Å, while the C–$C_{(Ar)}$ bond length is 1.492 Å. The endocyclic N–C(O) bond is in the antiperiplanar conformation to the exocyclic C=O bond ($O_{(exo)}$–C–N–C angle of 139.89°); the exocyclic N–C(O) bond is in the eclipsed conformation to the ring C=O bond ($O_{(endo)}$–C–N–C angle of 1.26°). Interestingly, the endocyclic amide bond is not planar ($\tau$ = 13.1°, $\chi_N$ = 22.2°, $\chi_C$ = 1.4°), additive Winkler-Dunitz distortion parameter $\Sigma(\tau+\chi_N)$ of 35.2°, which corresponds to approximately 24% the maximum theoretical distortion of the amide bond. In this case, the major geometric factor contributing to the distortion is N-pyramidalization vs. twist along the N–C(O) axis. The amide bond lengths in the six-membered ring are N–C(O) of 1.396 Å and C=O of 1.218 Å, respectively. Overall, these values indicate significant distortion of the exocyclic amide bond leading to the high selectivity in amide N–C(O) bond cleavage reactions. The cleavage of the alternative endocyclic N–C(O) bond is not observed due to insufficient alteration of $n_N \rightarrow \pi^*_{C=O}$ conjugation.

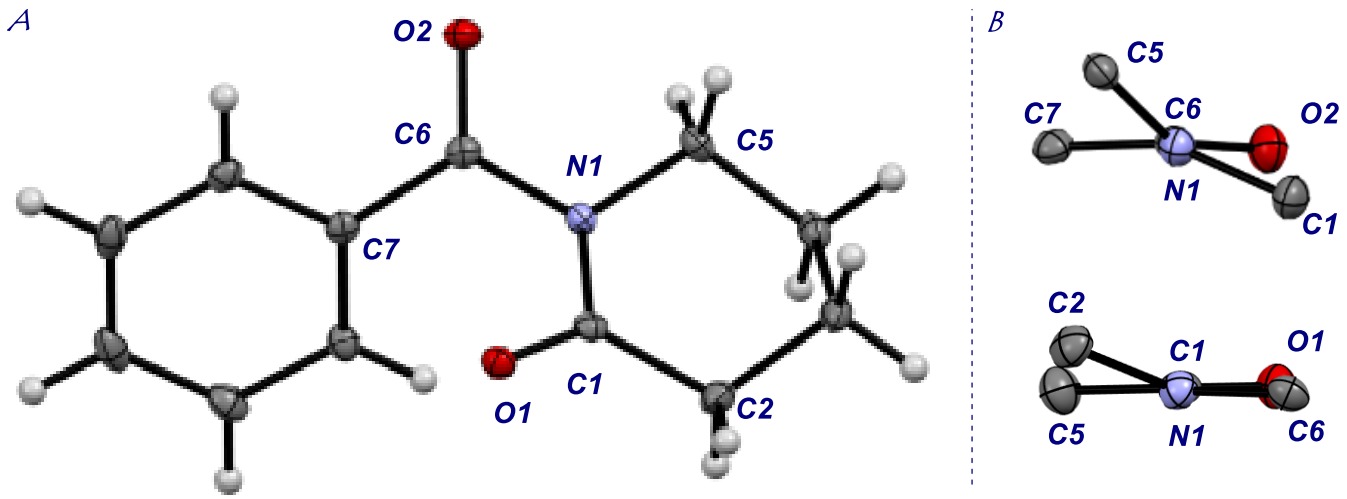

**Figure 3.** (a) Crystal structure of **2a**. 50% ellipsoids. (b) Projection of the amide group: N–C(O) bond (PhCO–, top; lactam, bottom). Note that projections represent views along N–C bonds illustrating distortion of the respective C–N–C(O)–C and C–C–C(O)–O torsions from planarity. For planar amides the respective dihedral angles are 0°. The structure has been deposited with the Cambridge Crystallographic Data Center, CCDC, 2082397. Bond lengths (Å) and angles (deg): N1–C6, 1.408(1); C6–O2, 1.216(1); C7–C6, 1.492(2); N1–C1, 1.396(1); C1–O1, 1.218(1), C1–C2, 1.505(2); C7–C6–N1–C5, 153.7(1); O2–C6–N1–C1, 139.9(1); O2–C6–N1–C5, –19.3(2); C7–C6–N1–C1, –47.1(1); C2–C1–N1–C6, 177.3(1); O1–C1–N1–C5, 156.6(1); O1–C1–N1–C6, –1.3(2); C2–C1–N1–C5, –24.8(2). Note weaker N1–C6(O) than N1–C1(O) bond.

**Computational studies.** Computational studies were conducted to probe the energetic properties of the amide bond in N-acyl-δ-valerolactams and determine the effect of mono-acyl amide activation (Scheme 5). We have employed the COSNAR method[14a,b] to determine resonance energies of the exo- and endocyclic amide bonds in N-benzoyl-δ-valerolactam (**2a**) according to eq 1.

$$-RE = E_{T(amide)} - [E_{T(amine)} + E_{T(ketone)} - E_{T(hydrocarbon)}] \quad \text{(eq. 1)}$$

B3LYP/6-311++G(d,p) level was selected to perform geometry optimization due to good reproducibility of literature data and method practicality. Extensive studies have demonstrated that this level is accurate in predicting structural and energetic properties of amides.[11,12,16] The method was further verified by obtaining good correlation between the calculated structure and the X-ray structure in this series. Calculated distortion parameters for **2a** are ($\tau$ = 30.3°, $\chi_N$ = 21.1°, $\chi_C$ = 5.4°; $\Sigma(\tau+\chi_N)$ of 51.4°), which can be compared with the x-ray determined values of ($\tau$ = 33.2°, $\chi_N$ = 20.8°, $\chi_C$ = 7.0°; $\Sigma(\tau+\chi_N)$ of 54.0°). (1) Thus, resonance energy showed that amidic resonance of the exo-cyclic amide bond in **2a** (RE = 5.6 kcal/mol) is significantly lower than in planar amides (18.3 kcal/mol for DMAc calculated at the same level),[11b] while resonance energy of the endo-cyclic amide bond in **2a** (RE = 9.2

kcal/mol) confirms the energetic preference and high chemoselectivity for cross-coupling of the twisted amide bond. (2) Determination of rotational profile of the exo-cyclic amide bond in **2a** by systematic rotation along the O–C–N–$C_{(Ar)}$ dihedral angle identified the energy minimum at ca. 20° O–C–N–C angle ($\tau$ = 32.58°; $\chi_N$ = 20.08°) in the eclipsed conformation of the endocyclic amide bond ($O_{(endo)}$–C–N–C angle of 3.74°). The energy maximum is located at ca. 170° O–C– N–C dihedral angle ($\tau$ = 6.11°; $\chi_N$ = 10.51°, 9.15 kcal/mol) in a syn C=O/C=O conformation (26.56° O–C–N–$C_{(Me)}$ dihedral angle). (3) Further, determination of N-/O-protonation affinities (ΔPA) in **2a** indicated that the amide bond strongly favors protonation at the amide oxygen (ΔPA = 12.0 kcal/mol, exocyclic amide bond), while protonation at the oxygen atom of the endocyclic amide bond is slightly favored over O-protonation of the exocyclic amide bond (ΔPA = 13.5 kcal/mol, endocyclic amide bond).[16c,23] N-/O-protonation affinities (ΔPA) have been determined according to ref. 14a,b. Additional studies on N-/O-protonation affinities in non-planar amides have been published.[14c,d,16c] Thus, O-protonation of the lactam oxygen would facilitate activation of the exocyclic amide bond by enhanced $n_N \rightarrow \pi^*_{C=O}$ resonance.[24] Overall, the energetic parameters of the amide bond in **2a** validate the high selectivity observed in the activation of the exocyclic N–C(O) bond and provide the basis for the use of N-acyl-δ-valerolactams as effective electrophiles in acyl and decarbonylative pathways by N–C(O) activation.[4–10]

**Scheme 5. A) Resonance Energies, B) Proton Affinities of Amide Bonds in 2a**

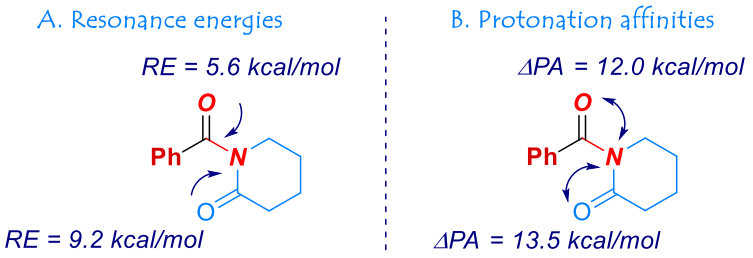

## 3. Conclusions

In summary, we have reported a comparative evaluation of cyclic amides as activating groups in N–C(O) cross-coupling. Most crucially, the study resulted in the determination of the relative reactivity order of N-acyl-imides, N-acyl-lactams, and N-acyl-oxazolidinones bearing five- and six-membered rings as activating groups for N–C(O) cross-coupling and the discovery of N-acyl-δ-valerolactams as a highly effective class of mono-N-acyl-activated amide precursors in cross-coupling. Furthermore, representative phenolic esters and thioesters have been evaluated in O–C(O) and S–C(O) cross-coupling under the same reaction conditions. The cross-coupling of N-acyl-δ-valerolactams proceeds with high selectivity for the exocyclic amide bond, including broad substrate scope. Determination of the x-ray structure of the parent N-benzoyl-δ-valerolactam demonstrated that the amide bond is characterized by the additive Winkler-Dunitz distortion parameter $\Sigma(\tau+\chi_N)$ of 54.0°, which results in a medium distortion range of twisted amides. Computational studies provided insight into the energetic parameters of the amide bond in N-benzoyl-δ-valerolactam and verified significantly reduced amidic resonance in the exocyclic amide bond. The reactivity of N-acyl- δ-valerolactams will represent a valuable addition to the portfolio of electrophilic cross-coupling reagents by N–C(O) bond activation, while these reagents should be added to the routine toolbox of amide bond derivatives for new reaction screening and optimization. Mechanistic studies, including on the effect of the oxidative addition using different amide derivatives with metal–NHC systems, are ongoing. Further studies on amide bond activation are underway in our laboratories and will be reported in due course.

## Experimental Section

**General Methods.** All compounds reported in the manuscript have been previously described in literature or prepared by the method reported previously unless stated otherwise. All boronic acids are commercially available and have been purchased from Oakwood Chemical. All experiments involving palladium were performed using standard Schlenk techniques under nitrogen or argon unless stated otherwise. All solvents were purchased at the highest commercial grade and used as received or after

purification by distillation from sodium/benzophenone under nitrogen. All solvents were deoxygenated prior to use. All other chemicals were purchased at the highest commercial grade and used as received. All other general methods have been published.[7a] $^{1}H$ NMR and $^{13}C$ NMR data are given for all compounds in the Supporting Experimental for characterization purposes. $^{1}H$ NMR, $^{13}C$ NMR and HRMS data are reported for all new compounds.

**General Procedure for the Synthesis of Amides.** An oven-dried round-bottomed flask equipped with a stir bar was charged with an amine substrate (typically, 2.0-10.0 mmol, 1.0 equiv), 4-(dimethylamino)pyridine (0.1 equiv), triethylamine (1.5 equiv), and dichloromethane (0.1 M). Benzoyl chloride (1.1 equiv) was added dropwise to the reaction mixture with vigorous stirring at 0 °C, and the reaction mixture was stirred for 15 h at room temperature. After the indicated time, the reaction mixture was quenched with aqueous HCl (1.0 N, 10 mL), extracted with dichloromethane (2 x 15 mL), the combined organic layers were dried and concentrated under reduced pressure. Purification by column chromatography on silica gel (hexanes/ethyl acetate = 4:1) afforded the title products.

**General Procedure for the Synthesis of Esters.** A round-bottomed flask equipped with a stir bar was charged with a phenol substrate (10.0 mmol, 1.0 equiv) dissolved in water (1-2 mL), and benzoyl chloride (15.0 mmol 1.5 equiv) was added with vigorous stirring. Aqueous solution of NaOH (1.0 *N*, 10 mL, 10.0 mmol) was added dropwise with vigorous stirring, and the reaction mixture was stirred for 15 h at room temperature. After the indicated time, the reaction mixture was extracted with dichloromethane (2 x 20 mL). The combined organic layers were dried and concentrated under reduced pressure to afford the title products.

**General Procedure for Suzuki-Miyaura Cross-Coupling Catalyzed by [Pd(IPr)(cin)Cl].** An oven-dried reaction flask equipped with a stir bar was charged with an amide or ester substrate (0.10 mmol, 1.0 equiv), boronic acid (0.20 mmol, 2.0 equiv), $K_2CO_3$ (0.30 mmol, 3.0 equiv) and [Pd(IPr)(cin)Cl] (1.0 mol%), placed under a positive pressure of argon, and subjected to three evacuation/backfilling cycles under high vacuum. THF (0.25 M) was added with vigorous stirring at

room temperature, the reaction mixture was placed in a preheated oil bath at 60 °C and stirred for the 15 h. After the indicated time, the reaction mixture was cooled down to room temperature, diluted with $CH_2Cl_2$ (10 mL), filtered, and concentrated. A sample was analyzed by $^1H$ NMR ($CDCl_3$, 500 MHz) and/or GC-MS to obtain conversion, selectivity and yield using internal standard and comparison with authentic samples. Purification by chromatography on silica gel (hexanes/ethyl acetate = 10:1) afforded the title products.

**General Procedure for Suzuki-Miyaura Cross-Coupling Catalyzed by Pd-PEPPSI-IPr.** An oven-dried reaction flask equipped with a stir bar was charged with an amide or ester substrate (0.10 mmol, 1.0 equiv), boronic acid (0.20 mmol, 2.0 equiv), $K_2CO_3$ (0.30 mmol, 3.0 equiv) and Pd-PEPPSI-IPr (1.0 mol%), placed under a positive pressure of argon, and subjected to three evacuation/backfilling cycles under high vacuum. THF (0.25 M) was added with vigorous stirring at room temperature, the reaction mixture was placed in a preheated oil bath at 60 °C and stirred for the 15 h. After the indicated time, the reaction mixture was cooled down to room temperature, diluted with $CH_2Cl_2$ (10 mL), filtered, and concentrated. A sample was analyzed by $^1H$ NMR ($CDCl_3$, 500 MHz) and/or GC-MS to obtain conversion, selectivity and yield using internal standard and comparison with authentic samples.

**General Procedure for Suzuki-Miyaura Cross-Coupling Catalyzed by $[Pd(PCy_3)_2Cl_2]$.** An oven-dried vial equipped with a stir bar was charged with an amide or ester substrate (0.10 mmol, 1.0 equiv), boronic acid (0.20 mmol, 2.0 equiv), $Na_2CO_3$ (0.25 mmol, 2.5 equiv) and $[Pd(PCy_3)_2Cl_2]$ (3.0 mol%), placed under a positive pressure of argon, and subjected to three evacuation/backfilling cycles under high vacuum. THF (0.25 M) was added with vigorous stirring at room temperature, the reaction mixture was placed in a preheated oil bath at 120 °C and stirred for the 15 h. After the indicated time, the reaction mixture was cooled down to room temperature, diluted with $CH_2Cl_2$ (10 mL), filtered, and concentrated. A sample was analyzed by $^1H$ NMR ($CDCl_3$, 500 MHz) and/or GC-MS to obtain conversion, selectivity and yield using internal standard and comparison with authentic samples.

**General Procedure for Suzuki-Miyaura Cross-Coupling Catalyzed by $Pd(OAc)_2/PCy_3$.** An oven-dried vial equipped with a stir bar was charged with an amide or ester substrate (0.10 mmol, 1.0 equiv), boronic acid (0.20 mmol, 2.0 equiv), $Na_2CO_3$ (0.25 mmol, 2.5 equiv), $Pd(OAc)_2$ (3.0 mol%) and $PCy_3HBF_4$ (12.0 mol%), placed under a positive pressure of argon, and subjected to three evacuation/backfilling cycles under high vacuum. THF (0.25 M) was added with vigorous stirring at room temperature, the reaction mixture was placed in a preheated oil bath at 120 °C and stirred for the 15 h. After the indicated time, the reaction mixture was cooled down to room temperature, diluted with $CH_2Cl_2$ (10 mL), filtered, and concentrated. A sample was analyzed by $^1H$ NMR ($CDCl_3$, 500 MHz) and/or GC-MS to obtain conversion, selectivity and yield using internal standard and comparison with authentic samples.

**Representative Procedure for Suzuki-Miyaura Cross-Coupling. 1.0 mmol Scale.** An oven-dried vial equipped with a stir bar was charged with 1-benzoylpiperidin-2-one (203 mg, 1.0 mmol, 1.0 equiv), 4-tolyl-boronic acid (272 mg, 2.0 mmol, 2.0 equiv), $K_2CO_3$ (414 mg, 3.0 mmol, 3.0 equiv) and [Pd(IPr)(cin)Cl] (1.0 mol%), placed under a positive pressure of argon, and subjected to three evacuation/backfilling cycles under high vacuum. THF (4.0 mL, 0.25 M) was added with vigorous stirring at room temperature, the reaction mixture was placed in a preheated oil bath at 60 °C and stirred for 15 h. After the indicated time, the reaction mixture was cooled down to room temperature, diluted with $CH_2Cl_2$ (15 mL), filtered and concentrated. Purification by chromatography on silica gel (hexanes/ethyl acetate = 10:1) afforded the title product. Yield 94% (185 mg).

Compounds **1**,[4a] **2a**,[25] **2d**,[25] **3**,[4a] **4**,[27] **5**,[26] **6**,[26] **7**,[28] **8**,[10o] **9**[29] and **10**[18] have been previously reported in the literature. Spectroscopic properties matched literature data. Amides **2b**, **2c**, **2e**, **2f**, **2g** and **2h** are new compounds.

**1-Benzoylpiperidine-2,6-dione (1).** Yield 81% (1.76 g). White solid. **$^1H$ NMR (500 MHz, $CDCl_3$)** $\delta$ 7.90 – 7.81 (m, 2H), 7.63 (t, $J$ = 7.5 Hz, 1H), 7.48 (t, $J$ = 7.8 Hz, 2H), 2.74 (t, $J$ = 6.6 Hz, 4H), 2.10

(quint, $J$ = 6.6 Hz, 2H). **$^{13}C\{^{1}H\}$ NMR (125 MHz, $CDCl_3$)** $\delta$ 172.3, 171.1, 135.3, 132.0, 130.4, 129.4, 32.6, 17.7.

**1-Benzoylpiperidin-2-one (2a).** Yield 75% (1.52 g). White solid. **$^{1}H$ NMR (500 MHz, $CDCl_3$)** δ 7.55 (d, $J$ = 7.4 Hz, 2H), 7.47 (t, $J$ = 7.4 Hz, 1H), 7.38 (t, $J$ = 7.6 Hz, 2H), 3.80 (t, $J$ = 5.7 Hz, 2H), 2.56 (t, $J$ = 6.5 Hz, 2H), 2.00 – 1.92 (m, 4H). **$^{13}C\{^{1}H\}$ NMR (126 MHz, $CDCl_3$)** δ 175.0, 173.8, 136.5, 131.8, 128.4, 128.2, 46.4, 35.0, 23.2, 21.8.

**1-(4-Methylbenzoyl)piperidin-2-one (2b).** Yield 80% (0.87 g). White solid. **Mp** = 128 – 129 °C. **$^{1}H$ NMR (500 MHz, $CDCl_3$)** δ 7.47 (d, $J$ = 8.1 Hz, 2H), 7.18 (d, $J$ = 7.9 Hz, 2H), 3.78 (t, $J$ = 5.7 Hz, 2H), 2.56 (t, $J$ = 6.4 Hz, 2H), 2.37 (s, 3H), 1.99 – 1.91 (m, 4H). **$^{13}C\{^{1}H\}$ NMR (126 MHz, $CDCl_3$)** δ 176.0, 173.8, 142.5, 133.5, 129.2, 128.5, 46.5, 34.9, 23.2, 21.9, 21.8. **HRMS (ESI)** m/z: $[M + H]^+$ Calcd for $C_{13}H_{16}NO_2$ 218.1176; Found 218.1175.

**1-(4-Methoxybenzoyl)piperidin-2-one (2c).** Yield 77% (0.89 g). White solid. **Mp** = 100 – 101 °C. **$^{1}H$ NMR (500 MHz, $CDCl_3$)** δ 7.57 (d, $J$ = 8.9 Hz, 2H), 6.87 (d, $J$ = 8.9 Hz, 2H), 3.83 (s, 3H), 3.75 (t, $J$ = 5.7 Hz, 2H), 2.56 (t, $J$ = 6.4 Hz, 2H), 1.98 – 1.91 (m, 4H). **$^{13}C\{^{1}H\}$ NMR (126 MHz, $CDCl_3$)** δ 174.5, 173.8, 163.0, 131.0, 128.3, 113.8, 55.7, 46.6, 34.9, 23.2, 21.8. **HRMS (ESI)** m/z: $[M + H]^+$ Calcd for $C_{13}H_{16}NO_3$ 234.1125; Found 234.1124.

**1-(4-(Trifluoromethyl)benzoyl)piperidin-2-one (2d).** Yield 74% (1.00 g). White solid. **$^{1}H$ NMR (500 MHz, $CDCl_3$)** δ 7.64 (d, $J$ = 8.3 Hz, 2H), 7.59 (d, $J$ = 8.2 Hz, 2H), 3.82 (t, $J$ = 5.8 Hz, 2H), 2.56 (t, $J$ = 6.5 Hz, 2H), 2.02 – 1.90 (M, 4H). **$^{13}C\{^{1}H\}$ NMR (126 MHz, $CDCl_3$)** δ 173.8, 173.6, 140.2, 132.9 (q, $J^F$ = 32.7 Hz), 128.1, 125.5 (q, $J^F$ = 3.8 Hz), 124.0 (q, $J^F$ = 272.9 Hz), 46.4, 35.0, 23.0, 21.6. **$^{19}F$ NMR (471 MHz, $CDCl_3$)** δ -62.97 (s).

**Methyl 4-(2-oxopiperidine-1-carbonyl)benzoate (2e).** Yield 70% (0.36 g). White solid. **Mp** = 119 – 120 °C. **$^{1}H$ NMR (500 MHz, $CDCl_3$)** δ 8.05 (d, $J$ = 8.5 Hz, 2H), 7.55 (d, $J$ = 8.5 Hz, 2H), 3.92 (s, 3H), 3.82 (t, $J$ = 5.8 Hz, 2H), 2.56 (t, $J$ = 6.6 Hz, 2H), 2.01 – 1.92 (m, 4H). **$^{13}C\{^{1}H\}$ NMR (126 MHz,**

**$CDCl_3$)** δ 174.0, 173.7, 166.6, 140.8, 132.5, 129.8, 127.7, 52.6, 46.3, 35.0, 23.1, 21.7. **HRMS (ESI)** m/z: $[M + H]^+$ Calcd for $C_{14}H_{16}NO_4$ 262.1074; Found 262.1074.

**1-(2-Methylbenzoyl)piperidin-2-one (2f).** Yield 73% (0.79 g). Colorless oil. **$^1$H NMR (500 MHz, $CDCl_3$)** δ 7.17 – 7.12 (m, 1H), 7.07 (d, *J* = 7.8 Hz, 1H), 7.04 (d, *J* = 3.7 Hz, 2H), 3.70 (t, *J* = 6.0 Hz, 2H), 2.33 (t, *J* = 6.7 Hz, 2H), 2.23 (s, 3H), 1.80 – 1.69 (m, 4H). **$^{13}$C{$^1$H} NMR (126 MHz, $CDCl_3$)** δ 173.8, 172.7, 138.0, 134.5, 130.4, 129.3, 125.6, 125.4, 44.9, 34.5, 22.6, 20.9, 19.4. **HRMS (ESI)** m/z: $[M + H]^+$ Calcd for $C_{13}H_{16}NO_2$ 218.1176; Found 218.1174.

**1-([1,1'-Biphenyl]-4-carbonyl)piperidin-2-one (2g).** Yield 70% (0.39 g). White solid. **Mp** = 147 – 148 °C. **$^1$H NMR (500 MHz, $CDCl_3$)** δ 7.68 – 7.55 (m, 6H), 7.45 (t, *J* = 7.6 Hz, 2H), 7.37 (t, *J* = 7.3 Hz, 1H), 3.83 (t, *J* = 5.7 Hz, 2H), 2.60 (t, *J* = 6.5 Hz, 2H), 2.03 – 1.94 (m, 4H). **$^{13}$C{$^1$H} NMR (126 MHz, $CDCl_3$)** δ 174.8, 173.9, 144.8, 140.6, 135.1, 129.2, 128.9, 128.2, 127.6, 127.2, 46.6, 35.0, 23.2, 21.8. **HRMS (ESI)** m/z: $[M + H]^+$ Calcd for $C_{18}H_{18}NO_2$ 280.1332; Found 280.1329.

**1-(Furan-2-carbonyl)piperidin-2-one (2h).** Yield 72% (0.56 g). White solid. **Mp** = 58 – 59 °C. **$^1$H NMR (500 MHz, $CDCl_3$)** δ 7.44 (d, *J* = 0.8 Hz, 1H), 7.10 (d, *J* = 3.5 Hz, 1H), 6.46 (dd, *J* = 3.5, 1.7 Hz, 1H), 3.71 (t, *J* = 4.5 Hz, 2H), 2.57 (dd, *J* = 8.3, 4.9 Hz, 2H), 1.93 – 1.90 (m, 4H). **$^{13}$C{$^1$H} NMR (126 MHz, $CDCl_3$)** δ 173.4, 163.8, 148.7, 145.3, 117.9, 112.2, 46.4, 34.8, 23.0, 21.9. **HRMS (ESI)** m/z: $[M + H]^+$ Calcd for $C_{10}H_{12}NO_3$ 194.0812; Found 194.0812.

**1-Benzoylpyrrolidine-2,5-dione (3).** Yield 75% (1.52 g). White solid. **$^1$H NMR (500 MHz, $CDCl_3$)** δ 7.84 (d, *J* = 7.3 Hz, 2H), 7.65 (t, *J* = 7.5 Hz, 1H), 7.49 (t, *J* = 7.9 Hz, 2H), 2.91 (s, 4H). **$^{13}$C{$^1$H} NMR (126 MHz, $CDCl_3$)** δ 175.0, 168.0, 135.4, 131.7, 130.8, 129.3, 29.4.

**2-Benzoylisoindoline-1,3-dione (4).** Yield 80% (2.00 g). White solid. **$^1$H NMR (500 MHz, $CDCl_3$)** δ 8.03 – 7.95 (m, 2H), 7.91 – 7.83 (m, 4H), 7.66 (t, *J* = 7.5 Hz, 1H), 7.50 (t, *J* = 7.8 Hz, 2H). **$^{13}$C{$^1$H} NMR (126 MHz, $CDCl_3$)** δ 167.4, 165.9, 135.6, 134.8, 132.9, 131.8, 130.8, 129.0, 124.8.

**1-Benzoylpyrrolidin-2-one (5).** Yield 62% (0.59 g). White solid. **$^{1}$H NMR (500 MHz, $CDCl_3$)** δ 7.60 (d, *J* = 7.2 Hz, 2H), 7.51 (t, *J* = 7.5 Hz, 1H), 7.40 (t, *J* = 7.7 Hz, 2H), 3.95 (t, *J* = 7.1 Hz, 2H), 2.59 (t, *J* = 8.0 Hz, 2H), 2.16 – 2.10 (m, 2H). **$^{13}$C{$^{1}$H} NMR (126 MHz, $CDCl_3$)** δ 174.8, 171.0, 134.7, 132.2, 129.2, 128.1, 46.8, 33.6, 17.9.

**3-Benzoyloxazolidin-2-one (6).** Yield 77% (0.74 g). White solid. **$^{1}$H NMR (500 MHz, $CDCl_3$)** δ 7.66 (d, *J* = 7.2 Hz, 2H), 7.55 (t, *J* = 7.5 Hz, 1H), 7.43 (t, *J* = 7.7 Hz, 2H), 4.47 (t, *J* = 7.8 Hz, 2H), 4.16 (t, *J* = 7.8 Hz, 2H). **$^{13}$C{$^{1}$H} NMR (126 MHz, $CDCl_3$)** δ 170.1, 153.5, 132.9, 132.7, 129.4, 128.2, 62.6, 44.0.

**3-Benzoylbenzo[*d*]oxazol-2(3H)-one (7).** Yield 75% (0.90 g). White solid. **$^{1}$H NMR (500 MHz, $CDCl_3$)** δ 7.88 – 7.84 (m, 1H), 7.84 – 7.77 (m, 2H), 7.65 (t, *J* = 7.5 Hz, 1H), 7.51 (t, *J* = 7.8 Hz, 2H), 7.31 – 7.25 (m, 3H). **$^{13}$C{$^{1}$H} NMR (126 MHz, $CDCl_3$)** δ 168.1, 151.3, 143.1, 133.9, 132.4, 129.9, 128.7, 128.7, 125.6, 125.1, 115.4, 110.5.

**Pentafluorophenyl benzoate (8).** Yield 82% (1.18 g). White solid. **$^{1}$H NMR (500 MHz, $CDCl_3$)** δ 8.21 (d, *J* = 7.5 Hz, 2H), 7.71 (t, *J* = 7.4 Hz, 1H), 7.56 (t, *J* = 7.8 Hz, 2H). **$^{13}$C{$^{1}$H} NMR (126 MHz, $CDCl_3$)** δ 163.0, 142.9 – 142.3 (m), 141.3 – 140.6 (m), 139.5 – 139.2 (m), 139.2 – 138.7 (m), 137.6 – 137.1 (m), 135.1, 131.1, 129.3, 127.3, 126.0 – 125.5 (m). **$^{19}$F NMR (471 MHz, $CDCl_3$)** δ -152.47 – -152.58 (m), -158.04 (t , $J^F$ = 21.7 Hz), -162.30 – -162.86 (m).

**Phenyl benzoate (9).** Yield 85% (1.68 g). White solid. **$^{1}$H NMR (500 MHz, $CDCl_3$)** δ 8.29 – 8.22 (m, 2H), 7.66 (t, *J* = 7.4 Hz, 1H), 7.54 (t, *J* = 7.7 Hz, 2H), 7.49 – 7.44 (m, 2H), 7.34 – 7.29 (m, 1H), 7.29 – 7.23 (m, 2H). **$^{13}$C{$^{1}$H} NMR (126 MHz, $CDCl_3$)** δ 165.4, 151.2, 133.8, 130.4, 129.9, 129.8, 128.8, 126.2, 122.0.

**S-Phenyl benzothioate (10).** Yield 83% (1.78 g). White solid. **$^{1}$H NMR (500 MHz, $CDCl_3$)** δ 8.10 – 8.02 (m, 2H), 7.62 (t, *J* = 7.4 Hz, 1H), 7.55 (dt, *J* = 5.3, 2.0 Hz, 2H), 7.53 – 7.46 (m, 5H). **$^{13}$C{$^{1}$H} NMR (126 MHz, $CDCl_3$)** δ 190.4, 136.9, 135.4, 134.0, 129.8, 129.5, 129.0, 127.8, 127.7.

All products reported in this manuscript have been previously reported: **12a**,[4a] **12b**,[4a] **12c**,[9h] **12d**,[9h] **12e**,[9h] **12f**,[9h] **12g**,[30] **12h**,[9h] **12i**,[27] **12j**,[27] **12k**,[27] **12l**,[27] **12m**,[27] **12n**,[27] **12o**,[27] **12p**,[4a] **12q**[4a] and **12r**.[29] Spectroscopic data matched those reported in the literature.

**Phenyl(*p*-tolyl)methanone (12a).** According to the general procedure, the reaction of 1-benzoylpiperidin-2-one (20.3 mg, 0.10 mmol, 1.0 equiv) and *p*-tolylboronic acid (27.2 mg, 0.20 mmol, 2.0 equiv) afforded the title compound after workup and chromatography. Yield 89% (17.4 mg). White solid. **$^1$H NMR (500 MHz, $CDCl_3$)** δ 7.79 (d, *J* = 7.3 Hz, 2H), 7.73 (d, *J* = 8.1 Hz, 2H), 7.57 (t, *J* = 7.4 Hz, 1H), 7.47 (t, *J* = 7.6 Hz, 2H), 7.28 (d, *J* = 7.8 Hz, 2H), 2.44 (s, 3H). **$^{13}$C{$^1$H} NMR (126 MHz, $CDCl_3$)** δ 196.8, 143.5, 138.3, 135.2, 132.4, 130.6, 130.2, 129.3, 128.5, 21.9.

**Di-*p*-tolylmethanone (12b).** According to the general procedure, the reaction of 1-(4-methylbenzoyl)piperidin-2-one (21.7 mg, 0.10 mmol, 1.0 equiv) and *p*-tolylboronic acid (27.2 mg, 0.20 mmol, 2.0 equiv) afforded the title compound after workup and chromatography. Yield 95% (19.9 mg). White solid. **$^1$H NMR (500 MHz, $CDCl_3$)** δ 7.73 (d, *J* = 8.1 Hz, 4H), 7.30 (d, *J* = 7.9 Hz, 4H), 2.46 (s, 6H). **$^{13}$C{$^1$H} NMR (126 MHz, $CDCl_3$)** δ 196.5, 143.2, 135.5, 130.5, 129.2, 21.9.

**(4-Methoxyphenyl)(*p*-tolyl)methanone (12c).** According to the general procedure, the reaction of 1-(4-methoxybenzoyl)piperidin-2-one (23.3 mg, 0.10 mmol, 1.0 equiv) and *p*-tolylboronic acid (27.2 mg, 0.20 mmol, 2.0 equiv) afforded the title compound after workup and chromatography. Yield 96% (21.7). White solid. **$^1$H NMR (500 MHz, $CDCl_3$)** δ 7.83 (d, *J* = 8.9 Hz, 2H), 7.70 (d, *J* = 8.1 Hz, 2H), 7.29 (d, *J* = 8.0 Hz, 2H), 6.98 (d, *J* = 8.9 Hz, 2H), 3.90 (s, 3H), 2.46 (s, 3H). **$^{13}$C{$^1$H} NMR (126 MHz, $CDCl_3$)** δ 195.6, 163.4, 142.9, 135.8, 132.7, 130.8, 130.3, 129.2, 113.8, 55.8, 21.9.

***p*-Tolyl(4-(trifluoromethyl)phenyl)methanone (12d).** According to the general procedure, the reaction of 1-(4-(trifluoromethyl)benzoyl)piperidin-2-one (27.1 mg, 0.10 mmol, 1.0 equiv) and *p*-tolylboronic acid (27.2 mg, 0.20 mmol, 2.0 equiv) afforded the title compound after workup and chromatography. Yield 96% (25.3 mg). White solid. **$^1$H NMR (500 MHz, $CDCl_3$)** δ 7.87 (d, *J* = 8.1 Hz,

2H), 7.73 (dd, $J$ = 13.5, 8.1 Hz, 4H), 7.31 (d, $J$ = 7.9 Hz, 2H), 2.46 (s, 3H). **$^{13}C\{^1H\}$ NMR (126 MHz, $CDCl_3$)** δ 195.6, 144.4, 141.5, 134.4, 133.9 (q, $J^F$ = 32.7 Hz), 130.7, 130.4, 129.6, 125.6 (q, $J^F$ = 3.7 Hz), 124.1 (q, $J^F$ = 273.1 Hz), 22.1. **$^{19}F$ NMR (471 MHz, $CDCl_3$)** δ -62.97 (s).

**Methyl 4-(4-methylbenzoyl)benzoate (12e).** According to the general procedure, the reaction of methyl 4-(2-oxopiperidine-1-carbonyl)benzoate (26.1 mg, 0.10 mmol, 1.0 equiv) and *p*-tolylboronic acid (27.2 mg, 0.20 mmol, 2.0 equiv) afforded the title compound after workup and chromatography. Yield 93% (23.6 mg). White solid. **$^1H$ NMR (500 MHz, $CDCl_3$)** δ 8.14 (d, $J$ = 8.5 Hz, 2H), 7.81 (d, $J$ = 8.5 Hz, 2H), 7.71 (d, $J$ = 8.1 Hz, 2H), 7.30 (d, $J$ = 7.9 Hz, 2H), 3.96 (s, 3H), 2.45 (s, 3H). **$^{13}C\{^1H\}$ NMR (126 MHz, $CDCl_3$)** δ 196.1, 166.7, 144.2, 142.1, 134.6, 133.4, 130.7, 130.0, 129.8, 129.5, 52.8, 22.0.

***o*-Tolyl(*p*-tolyl)methanone (12f).** According to the general procedure, the reaction of 1-(2-methylbenzoyl)piperidin-2-one (20.3 mg, 0.10 mmol, 1.0 equiv) and *p*-tolylboronic acid (27.2 mg, 0.20 mmol, 2.0 equiv) afforded the title compound after workup and chromatography. Yield 94% (19.7 mg). White solid. **$^1H$ NMR (500 MHz, $CDCl_3$)** δ 7.74 (d, $J$ = 8.2 Hz, 2H), 7.40 (td, $J$ = 7.5, 1.4 Hz, 1H), 7.34 – 7.24 (m, 5H), 2.45 (s, 3H), 2.35 (s, 3H). **$^{13}C\{^1H\}$ NMR (126 MHz, $CDCl_3$)** δ 198.7, 144.4, 139.3, 136.8, 135.5, 131.2, 130.6, 130.3, 129.5, 128.6, 125.5, 22.0, 20.2.

**[1,1'-Biphenyl]-4-yl(*p*-tolyl)methanone (12g).** According to the general procedure, the reaction of 1-([1,1'-biphenyl]-4-carbonyl)piperidin-2-one (27.9 mg, 0.10 mmol, 1.0 equiv) and *p*-tolylboronic acid (27.2 mg, 0.20 mmol, 2.0 equiv) afforded the title compound after workup and chromatography. Yield 92% (25.0 mg). White solid. **$^1H$ NMR (500 MHz, $CDCl_3$)** δ 7.88 (d, $J$ = 8.2 Hz, 2H), 7.76 (d, $J$ = 8.0 Hz, 2H), 7.70 (d, $J$ = 8.1 Hz, 2H), 7.66 (d, $J$ = 7.3 Hz, 2H), 7.49 (t, $J$ = 7.5 Hz, 2H), 7.41 (t, $J$ = 7.4 Hz, 1H), 7.31 (d, $J$ = 7.9 Hz, 2H), 2.46 (s, 3H). **$^{13}C\{^1H\}$ NMR (126 MHz, $CDCl_3$)** δ 196.5, 145.3, 143.5, 140.4, 136.9, 135.4, 130.9, 130.6, 129.3, 129.3, 128.5, 127.6, 127.3, 22.0.

**Furan-2-yl(*p*-tolyl)methanone (12h).** According to the general procedure, the reaction of 1-(furan-2-carbonyl)piperidin-2-one (19.3 mg, 0.10 mmol, 1.0 equiv) and *p*-tolylboronic acid (27.2 mg, 0.20

mmol, 2.0 equiv) afforded the title compound after workup and chromatography. Yield 88% (16.4 mg). Colourless oil. **$^1$H NMR (500 MHz, $CDCl_3$)** δ 7.89 (d, *J* = 8.2 Hz, 2H), 7.68 (d, *J* = 0.9 Hz, 1H), 7.29 (d, *J* = 7.9 Hz, 2H), 7.21 (dd, *J* = 3.5, 0.5 Hz, 1H), 6.57 (dd, *J* = 3.5, 1.7 Hz, 1H), 2.43 (s, 3H). **$^{13}$C{$^1$H} NMR (126 MHz, $CDCl_3$)** δ 182.6, 152.8, 147.1, 143.7, 134.9, 129.8, 129.4, 120.4, 112.4, 21.9.

**Benzophenone (12i).** According to the general procedure, the reaction of 1-benzoylpiperidin-2-one (20.3 mg, 0.10 mmol, 1.0 equiv) and phenylboronic acid (24.4 mg, 0.20 mmol, 2.0 equiv) afforded the title compound after workup and chromatography. Yield 91% (16.6 mg). White solid. **$^1$H NMR (500 MHz, $CDCl_3$)** δ 7.81 (d, *J* = 7.2 Hz, 2H), 7.59 (t, *J* = 7.4 Hz, 1H), 7.49 (t, *J* = 7.7 Hz, 2H). **$^{13}$C{$^1$H} NMR (126 MHz, $CDCl_3$)** δ 197.1, 138.0, 132.8, 130.4, 128.6.

**(4-Methoxyphenyl)(phenyl)methanone (12j).** According to the general procedure, the reaction of 1-benzoylpiperidin-2-one (20.3 mg, 0.10 mmol, 1.0 equiv) and (4-methoxyphenyl)boronic acid (30.4 mg, 0.20 mmol, 2.0 equiv) afforded the title compound after workup and chromatography. Yield 97% (20.5 mg). White solid. **$^1$H NMR (500 MHz, $CDCl_3$)** δ 7.82 (d, *J* = 8.8 Hz, 2H), 7.75 (d, *J* = 7.1 Hz, 2H), 7.55 (t, *J* = 7.4 Hz, 1H), 7.46 (t, *J* = 7.6 Hz, 2H), 6.95 (d, *J* = 8.8 Hz, 2H), 3.86 (s, 3H). **$^{13}$C{$^1$H} NMR (126 MHz, $CDCl_3$)** δ 195.8, 163.5, 138.6, 132.8, 132.2, 130.4, 130.0, 128.5, 113.8, 55.7.

**Phenyl(4-(trifluoromethyl)phenyl)methanone (12k).** According to the general procedure, the reaction of 1-benzoylpiperidin-2-one (20.3 mg, 0.10 mmol, 1.0 equiv) and (4-(trifluoromethyl)phenyl)boronic acid (38.0 mg, 0.20 mmol, 2.0 equiv) afforded the title compound after workup and chromatography. Yield 87% (21.7 mg). White solid. **$^1$H NMR (500 MHz, $CDCl_3$)** δ 7.89 (d, *J* = 8.0 Hz, 2H), 7.80 (d, *J* = 8.1 Hz, 2H), 7.75 (d, *J* = 8.1 Hz, 2H), 7.63 (t, *J* = 7.4 Hz, 1H), 7.51 (t, *J* = 7.7 Hz, 2H). **$^{13}$C{$^1$H} NMR (126 MHz, $CDCl_3$)** δ 195.8, 141.1, 137.1, 134.0 (q, $J^F$ = 32.7 Hz), 133.4, 130.5, 130.4, 128.9, 125.7 (q, $J^F$ = 3.7 Hz), 124.0 (q, $J^F$ = 273.1 Hz). **$^{19}$F NMR (471 MHz, $CDCl_3$)** δ -63.00 (s).

**1-(4-Benzoylphenyl)ethan-1-one (12l).** According to the general procedure, the reaction of 1-benzoylpiperidin-2-one (20.3 mg, 0.10 mmol, 1.0 equiv) and (4-acetylphenyl)boronic acid (32.8 mg, 0.20 mmol, 2.0 equiv) afforded the title compound after workup and chromatography. Yield 82% (18.4 mg). White solid. **$^1$H NMR (500 MHz, $CDCl_3$)** δ 8.05 (d, *J* = 8.4 Hz, 2H), 7.86 (d, *J* = 8.4 Hz, 2H), 7.80 (d, *J* = 7.1 Hz, 2H), 7.62 (t, *J* = 7.4 Hz, 1H), 7.50 (t, *J* = 7.7 Hz, 2H), 2.66 (s, 3H). **$^{13}$C{$^1$H} NMR (126 MHz, $CDCl_3$)** δ 197.8, 196.3, 141.7, 139.9, 137.2, 133.3, 130.4, 130.4, 128.8, 128.5, 27.2.

**Methyl 4-benzoylbenzoate (12m).** According to the general procedure, the reaction of 1-benzoylpiperidin-2-one (20.3 mg, 0.10 mmol, 1.0 equiv) and (4-(methoxycarbonyl)phenyl)boronic acid (36.0 mg, 0.20 mmol, 2.0 equiv) afforded the title compound after workup and chromatography. Yield 82% (19.7 mg). White solid. **$^1$H NMR (500 MHz, $CDCl_3$)** δ 8.15 (d, *J* = 8.5 Hz, 2H), 7.84 (d, *J* = 8.5 Hz, 2H), 7.82 – 7.77 (m, 2H), 7.61 (t, *J* = 7.4 Hz, 1H), 7.50 (t, *J* = 7.7 Hz, 2H), 3.96 (s, 3H). **$^{13}$C{$^1$H} NMR (126 MHz, $CDCl_3$)** δ 196.4, 166.7, 141.7, 137.3, 133.6, 133.3, 130.5, 130.1, 129.9, 128.8, 52.8.

**Phenyl(*o*-tolyl)methanone (12n).** According to the general procedure, the reaction of 1-benzoylpiperidin-2-one (20.3 mg, 0.10 mmol, 1.0 equiv) and *o*-tolylboronic acid (27.2 mg, 0.20 mmol, 2.0 equiv) afforded the title compound after workup and chromatography. Yield 90% (17.7 mg). Colourless oil. **$^1$H NMR (500 MHz, $CDCl_3$)** δ 7.84 – 7.77 (m, 2H), 7.58 (t, *J* = 7.4 Hz, 1H), 7.46 (t, *J* = 7.7 Hz, 2H), 7.39 (td, *J* = 7.6, 1.1 Hz, 1H), 7.31 (dd, *J* = 11.7, 7.6 Hz, 2H), 7.25 (t, *J* = 7.25 Hz, 1H), 2.34 (s, 3H). **$^{13}$C{$^1$H} NMR (126 MHz, $CDCl_3$)** δ 198.9, 138.9, 138.1, 137.0, 133.4, 131.3, 130.5, 130.4, 128.8, 128.8, 125.5, 20.3.

**(2-Methoxyphenyl)(phenyl)methanone (12o).** According to the general procedure, the reaction of 1-benzoylpiperidin-2-one (20.3 mg, 0.10 mmol, 1.0 equiv) and (2-methoxyphenyl)boronic acid (30.4 mg, 0.20 mmol, 2.0 equiv) afforded the title compound after workup and chromatography. Yield 85% (18.0 mg). White solid. **$^1$H NMR (500 MHz, $CDCl_3$)** δ 7.82 (d, *J* = 7.1 Hz, 2H), 7.55 (t, *J* = 7.4 Hz, 1H), 7.49 – 7.40 (m, 3H), 7.36 (dd, *J* = 7.5, 1.6 Hz, 1H), 7.04 (td, *J* = 7.4, 0.6 Hz, 1H), 6.99 (d, *J* = 8.4 Hz, 1H),

3.71 (s, 3H). **$^{13}C\{^{1}H\}$ NMR (126 MHz, $CDCl_3$)** δ 196.7, 157.6, 138.1, 133.2, 132.2, 130.1, 129.8, 129.2, 128.5, 120.8, 111.8, 55.9.

**Naphthalen-1-yl(phenyl)methanone (12p).** According to the general procedure, the reaction of 1-benzoylpiperidin-2-one (20.3 mg, 0.10 mmol, 1.0 equiv) and naphthalen-1-ylboronic acid (34.4 mg, 0.20 mmol, 2.0 equiv) afforded the title compound after workup and chromatography. Yield 83% (19.3 mg). Colourless oil. **$^{1}H$ NMR (500 MHz, $CDCl_3$)** δ 8.10 (d, *J* = 8.2 Hz, 1H), 8.01 (d, *J* = 8.2 Hz, 1H), 7.93 (d, *J* = 7.6 Hz, 1H), 7.88 (d, *J* = 7.1 Hz, 2H), 7.62 – 7.57 (m, 2H), 7.56 – 7.49 (m, 3H), 7.46 (t, *J* = 7.8 Hz, 2H). **$^{13}C\{^{1}H\}$ NMR (126 MHz, $CDCl_3$)** δ 198.3, 138.6, 136.7, 134.0, 133.5, 131.6, 131.3, 130.7, 128.7, 128.7, 128.1, 127.6, 126.8, 126.0, 124.6.

**Naphthalen-2-yl(phenyl)methanone (12q).** According to the general procedure, the reaction of 1-benzoylpiperidin-2-one (20.3 mg, 0.10 mmol, 1.0 equiv) and naphthalen-2-ylboronic acid (34.4 mg, 0.20 mmol, 2.0 equiv) afforded the title compound after workup and chromatography. Yield 85% (19.7 mg). White solid. **$^{1}H$ NMR (500 MHz, $CDCl_3$)** δ 8.27 (s, 1H), 7.95 (d, *J* = 0.8 Hz, 2H), 7.92 (dd, *J* = 8.1, 3.0 Hz, 2H), 7.87 (d, *J* = 7.1 Hz, 2H), 7.65 – 7.60 (m, 2H), 7.55 (dt, *J* = 15.3, 4.2 Hz, 3H). **$^{13}C\{^{1}H\}$ NMR (126 MHz, $CDCl_3$)** δ 197.1, 138.2, 135.6, 135.1, 132.7, 132.6, 132.2, 130.4, 129.7, 128.7, 128.6, 128.6, 128.1, 127.1, 126.1.

**Furan-2-yl(phenyl)methanone (12r).** According to the general procedure, the reaction of 1-benzoylpiperidin-2-one (20.3 mg, 0.10 mmol, 1.0 equiv) and furan-2-ylboronic acid (22.4 mg, 0.20 mmol, 2.0 equiv) afforded the title compound after workup and chromatography. Yield 81% (13.9 mg). Colourless oil. **$^{1}H$ NMR (500 MHz, $CDCl_3$)** δ 7.96 (d, *J* = 7.1 Hz, 2H), 7.70 (d, *J* = 0.9 Hz, 1H), 7.58 (t, *J* = 7.4 Hz, 1H), 7.48 (t, *J* = 7.6 Hz, 2H), 7.22 (d, *J* = 3.6 Hz, 1H), 6.58 (dd, *J* = 3.5, 1.6 Hz, 1H). **$^{13}C\{^{1}H\}$ NMR (126 MHz, $CDCl_3$)** δ 182.9, 152.6, 147.4, 137.6, 132.9, 129.6, 128.7, 120.9, 112.5.

**Selectivity Studies Amides. General Procedure.** An oven-dried vial equipped with a stir bar was charged with two amide substrates (0.10 mmol, each), potassium carbonate (0.30 mmol), boronic acid

(0.05 mmol), [Pd(IPr)(cin)Cl] (1.0 mol%), placed under a positive pressure of argon, and subjected to three evacuation/backfilling cycles under high vacuum. THF (0.25 M) was added with vigorous stirring at room temperature, the reaction mixture was placed in a preheated oil bath at 60 °C and stirred for the 15 h. After the indicated time, the reaction mixture was cooled down to room temperature, diluted with $CH_2Cl_2$ (10 mL), filtered, and concentrated. A sample was analyzed by $^1H$ NMR ($CDCl_3$, 500 MHz) and/or GC-MS to obtain conversion, selectivity and yield using internal standard and comparison with authentic samples.

**Selectivity Studies Boronic Acids. General Procedure.** An oven-dried vial equipped with a stir bar was charged with an amide substrate (0.05 mmol), potassium carbonate (0.30 mmol), two boronic acid substrates (0.20 mmol, each), [Pd(IPr)(cin)Cl] (1.0 mol%), placed under a positive pressure of argon, and subjected to three evacuation/backfilling cycles under high vacuum. THF (0.25 M) was added with vigorous stirring at room temperature, the reaction mixture was placed in a preheated oil bath at 60 °C and stirred for the 15 h. After the indicated time, the reaction mixture was cooled down to room temperature, diluted with $CH_2Cl_2$ (10 mL), filtered, and concentrated. A sample was analyzed by $^1H$ NMR ($CDCl_3$, 500 MHz) and/or GC-MS to obtain conversion, selectivity and yield using internal standard and comparison with authentic samples.

**Details of Crystal Structure Analysis.** Crystallographic information is given in Table S1 in the Supporting Information. The compound was colorless single crystal. Full data sets were collected using graphite-monochromated CuKα radiation (λ = 1.54178 Å) on a Bruker SMART APEX2 single crystal diffractometer. X-rays were provided by a fine-focus sealed X-ray tube operated at 48kV and 30mA. Lattice constants were all determined using the Bruker SAINT software package using all available reflections. All data were corrected for absorption by measuring the faces of each crystal and doing a numerical absorption correction. The Bruker software package SHELXTL-2014 was used to solve all of the structures using the direct methods technique and difference electron density maps. All stages of weighted full-matrix least-squares refinement were conducted using $F_o^2$ data with the same software

package. The final structural model for each compound was refined using anisotropic thermal parameters for all non-hydrogen atoms; all of the H atoms were located in difference maps, but were placed in geometrically idealized positions and allowed to "ride" on their parent C, O or N atoms, with bond lengths of 0.95, 1.00, 0.99, 0.98, and 0.84 Å for aromatic, methine, methylene, methyl, and hydroxyl, respectively. The isotropic thermal parameters for these H atoms were fixed to be 1.2 times the $U_{iso}$ for C or N and 1.5 times the $U_{iso}$ for O.

**Supporting Information.** Cartesian coordinates and energies. Detailed description of computational methods used. CIF files for amide **2a**. This material is available free of charge via the Internet at http://pubs.acs.org.

**Author Information.** Corresponding author: michal.szostak@rutgers.edu

**Acknowledgements.** Rutgers University, the NSF (CAREER CHE-1650766, M.S.) and the NSF (CHE-1915878, H.C.) are gratefully acknowledged for support. The Bruker 500 MHz spectrometer was supported by the NSF-MRI grant (CHE-1229030). Additional support was provided by the Rutgers Graduate School in the form of Dean's Dissertation Fellowship (M. R.) and MBRS Undergraduate Fellowship (D. J. P.). We thank the Wroclaw Center for Networking and Supercomputing (grant no. WCSS159, R.S.).

**References**

(1) (a) Greenberg, A.; Breneman, C. M.; Liebman, J. F. *The Amide Linkage: Structural Significance in Chemistry, Biochemistry and Materials Science*; Wiley-VCH: New York, 2003. (b) Pattabiraman, V. R.; Bode, J. W. Rethinking Amide Bond Synthesis. *Nature* **2011**, *480*, 471-479. (c) Ruider, S.; Maulide, N. Strong Bonds Made Weak: Towards the General Utility of Amides as Synthetic Modules. *Angew. Chem. Int. Ed.* **2015**, *54*, 13856-13858.

(2) Pauling, L. *The Nature of the Chemical Bond*; Oxford University Press: London, 1940.

(3) For lead references on amide bonds in drug discovery and polymer chemistry, see: (a) Roughley, S. D.; Jordan, A. M. The Medicinal Chemist's Toolbox: An Analysis of Reactions Used in the Pursuit of Drug Candidates. *J. Med. Chem.* **2011**, *54*, 3451-3479. (b) Kaspar, A. A.; Reichert, J. M. Future Directions for Peptide Therapeutics Development. *Drug Discov. Today* **2013**, *18*, 807-817. (c) Marchildon, K. Polyamides: Still Strong After Seventy Years. *Macromol. React. Eng.* **2011**, *5*, 22-54. (d) Brunton, L.; Chabner, B.; Knollman, B. *Goodman and Gilman's The Pharmacological Basis of Therapeutics*; MacGraw-Hill: New York, 2010.

(4) For reviews on N–C functionalization, see: (a) Li, G.; Ma, S.; Szostak, M. Amide Bond Activation: The Power of Resonance. *Trends Chem.* **2020**, *2*, 914-928. (b) Shi, S.; Nolan, S. P.; Szostak, M. Well-Defined Palladium(II)-NHC (NHC = N-Heterocyclic Carbene) Precatalysts for Cross-Coupling Reactions of Amides and Esters by Selective Acyl CO–X (X = N, O) Cleavage. *Acc. Chem. Res.* **2018**, *51*, 2589-2599. (c) Liu, C.; Szostak, M. Decarbonylative Cross-Coupling of Amides. *Org. Biomol. Chem.* **2018**, *16*, 7998-8010. (d) Kaiser, D.; Bauer, A.; Lemmerer, M.; Maulide, N. Amide Activation: an Emerging Tool for Chemoselective Synthesis. *Chem. Soc. Rev.* **2018**, *47*, 7899-7925. (e) Dander, J. E.; Garg, N. K. Breaking Amides using Nickel Catalysis. *ACS Catal.* **2017**, *7*, 1413-1423. (f) Bourne-Branchu, Y.; Gosmini, C.; Danoun, G. N-Boc-Amides in Cross-Coupling Reactions. *Chem. Eur. J.* **2019**, *25*, 2663-2674. (g) Chaudhari, M. B.; Gnanaprakasam, B. Recent Advances in the Metal-Catalyzed Activation of Amide Bonds. *Chem. Asian J.* **2019**, *14*, 76-93.

(5) (a) Hie, L.; Nathel, N. F. F.; Shah, T. K.; Baker, E. L.; Hong, X.; Yang, Y. F.; Liu, P.; Houk, K. N.; Garg, N. K. Conversion of Amides to Esters by the Nickel-Catalysed Activation of Amide C–N Bonds. *Nature* **2015**, *524*, 79-83. (b) Weires, N. A.; Baker, E. L.; Garg, N. K. Nickel-catalysed Suzuki−Miyaura coupling of Amides. *Nature Chem.* **2016**, *8*, 76-80.

(6) Li, X.; Zou, G. Acylative Suzuki coupling of amides: acyl-nitrogen activation via synergy of independently modifiable activating groups. *Chem. Commun.* **2015**, *51*, 5089-5092.

(7) (a) Meng, G.; Szostak, M. Sterically-Controlled Pd-Catalyzed Chemoselective Ketone Synthesis via N–C Cleavage in Twisted Amides. *Org. Lett.* **2015**, *17*, 4364-4367. (b) Meng, G.; Szostak, M. General Olefin Synthesis by the Palladium-Catalyzed Heck Reaction of Amides: Sterically-Controlled Chemoselective N–C Activation. *Angew. Chem. Int. Ed.* **2015**, *54*, 14518-14522.

(8) For a review, see: Meng, G.; Szostak, M. N-Acyl-Glutarimides: Privileged Scaffolds in Amide N-C Bond Cross-Coupling. *Eur. J. Org. Chem.* **2018**, *20-21*, 2352-2365.

(9) For selected studies, see: (a) Ni, S.; Zhang, W.; Mei, H.; Han, J.; Pan, Y. Ni-Catalyzed Reductive Cross-Coupling of Amides with Aryl Iodide Electrophiles via C–N Bond Activation. *Org. Lett.* **2017**, *19*, 2536-2539. (b) Amani, J.; Alam, R.; Badir, S.; Molander, G. A. Synergistic Visible-Light Photoredox/Nickel-Catalyzed Synthesis of Aliphatic Ketones via N–C Cleavage of Imides. *Org. Lett.* **2017**, 19, 2426-2429. (c) Yue, H.; Guo, L.; Lee, S. C.; Liu, X.; Rueping, M. Selective Reductive Removal of Ester and Amide Groups from Arenes and Heteroarenes through Nickel-Catalyzed C–O and C–N Bond Activation. *Angew. Chem. Int. Ed.* **2017**, *56*, 3972-3976. (d) Srimontree, W.; Chatupheeraphat, A.; Liao, H. H.; Rueping, M. Amide to Alkyne Interconversion via a Nickel/Copper-Catalyzed Deamidative Cross-Coupling of Aryl and Alkenyl Amides. *Org. Lett.* **2017**, *19*, 3091-3094. (e) Guo, L.; Rueping, M. Decarbonylative Cross-Couplings: Nickel Catalyzed Functional Group Interconversion Strategies for the Construction of Complex Organic Molecules. *Acc. Chem. Res.* **2018**, *51*, 1185-1195. (f) Liu, L.; Zhou, D.; Liu, M.; Zhou, Y.; Chen, T. Palladium-Catalyzed Decarbonylative Alkynylation of Amides. *Org. Lett.* **2018**, *20*, 2741-2744. (g) Dorval, C.; Dubois, E.; Bourne-Branchu, Y.; Gosmini, C.; Danoun, G. Sequential Organozinc Formation and Negishi Cross-Coupling of Amides Catalysed by Cobalt Salt. *Adv. Synth. Catal.* **2019**, *361*, 1777-1780. (h) Idris, M. A.; Lee, S. Palladium-Catalyzed Amide N−C Hiyama Cross-Coupling: Synthesis of Ketones. *Org. Lett.* **2020**, *22*, 9190−9195. (i) For a recent pertinent example, see: Reina, A.; Krachko, T.; Onida, K.; Bouyssi, D.; Jeanneau, E.;

Monteiro, N.; Amgoune, A. Development and Mechanistic Investigations of a Base-Free Suzuki–Miyaura Cross-Coupling of α,α-Difluoroacetamides via C–N Bond Cleavage. *ACS Catal.* **2020**, *10*, 2189-2197.

(10) For further examples, see: (a) Li, C. X.; Ning, Q; Zhao, W.; Cao, H. J.; Wang, Y. P.; Yan, H.; Lu, C. S.; Liang, Y. Rh-Catalyzed Decarbonylative Cross-Coupling between o-Carboranes and Twisted Amides: A Regioselective, Additive-Free, and Concise Late-Stage Carboranylation. *Chem. Eur. J.* **2021**, *27*, 2699-2706. (b) Zhou, P. X.; Shi, S.; Wang, J.; Zhang, Y.; Li, C.; Ge, C. Palladium/Copper-Catalyzed Decarbonylative Heteroarylation of Amides via C–N Bond Activation. *Org. Chem. Front.* **2019**, *6*, 1942-1947. (c) Zhang, Y.; Wang, Z.; Tang, Z.; Luo, Z.; Wu, H.; Liu, T.; Zhu, Y.; Zeng, Z. Water Phase, Room Temperature, Ligand-Free Suzuki–Miyaura Cross-Coupling: A Green Gateway to Aryl Ketones by C–N Bond Cleavage. *Eur. J. Org. Chem.* **2020**, 1620-1628. (d) Cui, M.; Chen, Z.; Liu, T.; Wang, H.; Zeng, Z. N-Acylsuccinimides: Efficient Acylative Coupling Reagents in Palladium-Catalyzed Suzuki Coupling via C–N Cleavage. *Tetrahedron Lett.* **2017**, *58*, 3819-3822. (e) Wang, T.; Guo, J.; Wang, H.; Guo, H.; Jia, D.; Zhang, W.; Liu, L. N-Heterocyclic Carbene Palladium(II)-Catalyzed Suzuki-Miyaura Cross Coupling of N-Acylsuccinimides by C-N Cleavage. *J. Organomet. Chem.* **2018**, *877*, 80-84. (f) Lee, G. S.; Won, J.; Choi, S.; Baik, M.-H.; Hong, S. H. Synergistic Activation of Amides and Hydrocarbons for Direct C($sp^3$)–H Acylation Enabled by Metallaphotoredox Catalysis. *Angew. Chem., Int. Ed.* **2020**, *59*, 16933-16942. (g) Huang, Y.; Pan, W. -J.; Wang, Z. -X. Rhodium-Catalyzed Alkenyl C–H Functionalization with Amides. *Org. Chem. Front.* **2019**, *6*, 2284-2290. (h) Yu, C. -G.; Matsuo, Y. Nickel-Catalyzed Deaminative Acylation of Activated Aliphatic Amines with Aromatic Amides via C–N Bond Activation. *Org. Lett.* **2020**, *22*, 950-955. (i) Kerackian, T.; Reina, A.; Bouyssi, D.; Monteiro, N.; Amgoune, A. Silyl Radical Mediated Cross-Electrophile Coupling of N-Acyl-imides with Alkyl Bromides under Photoredox/Nickel Dual Catalysis. *Org. Lett.* **2020**, *22*, 2240-2245. (j) Jian, J.; He, Z.; Zhang, Y.; Liu, T.; Liu, L.; Wang, Z.; Wang, H.; Wang, S.; Zeng, Z. Palladium-Catalyzed Suzuki Coupling of N-Acyloxazolidinones via Selective Cleavage of C–

N Bonds. *Eur. J. Org. Chem.* **2020**, 4176-4180. (k) Huang, P. -Q.; Geng, H. Ni-Catalyzed Chemoselective Alcoholysis of N-Acyloxazolidinones. *Green Chem.* **2018**, *20*, 593-599. (l) Guissart, C.; Barros, A.; Barata, L. R.; Evano, G. Broadly Applicable Ytterbium-Catalyzed Esterification, Hydrolysis, and Amidation of Imides. *Org. Lett.* **2018**, *20*, 5098-5102. (m) Sibi, M. P.; Hasegawa, H.; Ghorpade, S. R. A Convenient Method for the Conversion of N-Acyloxazolidinones to Hydroxamic Acids. *Org. Lett.* **2002**, *4*, 3343-3346. (n) Tanii, S.; Arisawa, M.; Tougo, T.; Yamaguchi, M. Catalytic Method for the Synthesis of C−N-Linked Bi(heteroaryl)s Using Heteroaryl Ethers and N-Benzoyl Heteroarenes. *Org. Lett.* **2018**, *20*, 1756-1759. (o) Specklin, S.; Cossy, J. Chemoselective Synthesis of β-Ketophosphonates Using Lithiated α-(Trimethylsilyl)methylphosphonate. *J. Org. Chem.* **2015**, *80*, 3302-3308.

(11) For pertinent mechanistic studies on N-acyl-glutarimides, see: (a) Pace, V.; Holzer, W.; Meng, G.; Shi, S.; Lalancette, R.; Szostak, R.; Szostak, M. Structures of Highly Twisted Amides Relevant to Amide N−C Cross-Coupling: Evidence for Ground-State Amide Destabilization. *Chem. Eur. J.* **2016**, *22*, 14494-14498. (b) Szostak, R.; Szostak, M. N-Acyl-Glutarimides: Resonance and Proton Affinities of Rotationally-Inverted Twisted Amides Relevant to N−C(O) Cross-Coupling. *Org. Lett.* **2018**, *20*,1342-1345. For a structural comparison of amide derivatives, see: (c) Wang, C. A.; Liu, C.; Szostak, M. N-Acyl-5,5-Dimethylhydantoins: Mild Acyl-Transfer Reagents for the Synthesis of Ketones Using Pd–PEPPSI or Pd/Phosphine Catalysts. *Org. Process Res. Dev.* **2020**, *24*, 1043-1051. (d) Luo, Z.; Liu, T.; Guo, W.; Wang, Z.; Huang, J.; Zhu, Y.; Zeng, Z. *N*-Acyl-5,5-dimethylhydantoin, a New Mild Acyl-Transfer Reagent in Pd Catalysis: Highly Efficient Synthesis of Functionalized Ketones. *Org. Process Res. Dev.* **2018**, *22*, 1188-1199.

(12) Meng, G.; Shi, S.; Lalancette, R.; Szostak, R.; Szostak, M. Reversible Twisting of Primary Amides via Ground State N–C(O) Destabilization: Highly Twisted Rotationally Inverted Acyclic Amides. *J. Am. Chem. Soc.* **2018**, *140*, 727-734, and references cited therein.

(13) For representative studies on non-planar bridged lactams, see: (a) Tani, K.; Stoltz, B. M. Synthesis and structural analysis of 2-quinuclidonium tetrafluoroborate. *Nature* **2006**, *441*, 731-734. (b) Komarov, I. V.; Yanik, S.; Ishchenko, A. Y.; Davies, J. E.; Goodman, J. M.; Kirby, A. J. The Most Reactive Amide As a Transition-State Mimic For cis–trans Interconversion. *J. Am. Chem. Soc.* **2015**, *137*, 926-930. (c) Sliter, B.; Morgan, J.; Greenberg, A. 1-Azabicyclo[3.3.1]nonan-2-one: Nitrogen Versus Oxygen Protonation. *J. Org. Chem.* **2011**, *76*, 2770-2781. (d) Bennet, A. J.; Wang, Q. P.; Slebocka-Tilk, H.; Somayaji, V.; Brown, R. S.; Santarsiero, B. D. Relationship between amidic distortion and ease of hydrolysis in base. If amidic resonance does not exist, then what accounts for the accelerated hydrolysis of distorted amides? *J. Am. Chem. Soc.* **1990**, *112*, 6383-6385. (e) Lease, T. G.; Shea, K. J. The type 2 intramolecular imino Diels-Alder reaction. Synthesis and structural characterization of bicyclo[n.3.1] bridgehead olefin/bridgehead lactams. *J. Am. Chem. Soc.* **1993**, *115*, 2248-2260. (f) Bashore, C. G.; Samardjiev, I. J.; Bordner, J.; Coe, J. W. Twisted Amide Reduction under Wolff-Kishner Conditions: Synthesis of a Benzo-1-Aza-Adamantane Derivative. *J. Am. Chem. Soc.* **2003**, *125*, 3268-3272.

(14) For computational studies on bridged lactams, see: (a) Greenberg, A.; Venanzi, C. A. Structures and energetics of two bridgehead lactams and their N- and O-protonated forms: an ab initio molecular orbital study. *J. Am. Chem. Soc.* **1993**, *115*, 6951-6957. (b) Greenberg, A.; Moore, D. T.; DuBois, T. D. Small and Medium-Sized Bridgehead Bicyclic Lactams: A Systematic ab Initio Molecular Orbital Study. *J. Am. Chem. Soc.* **1996**, *118*, 8658-8668. (c) Morgan, J.; Greenberg, A. Novel bridgehead bicyclic lactams: Molecules predicted to have O-protonated and N-protonated tautomers of comparable stability; hyperstable lactams and their O-protonated tautomers. *J. Chem. Thermodynamics* **2014**, *73*, 206-212. (d) Szostak, R.; Aubé, J.; Szostak, M. Determination of Structures and Energetics of Small- and Medium-Sized One-Carbon Bridged Twisted Amides using ab Initio Molecular Orbital Methods. Implications for Amidic Resonance along the C–N Rotational Pathway. *J. Org. Chem.* **2015**, *80*, 7905-

7927. (e) For calculation of the Winkler-Dunitz parameters, see: Winkler, F. K.; Dunitz, J. D. The Non-Planar Amide Group. *J. Mol. Biol.* **1971**, *59*, 169-182.

(15) For recent studies of amide distortion by peripheral metal coordination, see: (a) Adachi, S.; Kumagai, N.; Shibasaki, M. Pyramidalization/twisting of the amide functional group via remote steric congestion triggered by metal coordination. *Chem. Sci.* **2017**, *8*, 85-90. (b) Adachi, S.; Kumagai, N.; Shibasaki, M. Bis(2-pyridyl)amides as Readily Cleavable Amides Under Catalytic, Neutral, and Room-Temperature Conditions. *Synlett* **2017**, *29*, 301-305. For an excellent perspective, see: Adachi, S.; Kumagai, N.; Shibasaki, M. Conquering amide planarity: Structural distortion and its hidden reactivity. *Tetrahedron Lett.* **2018**, *59*, 1147-1158.

(16) For further studies on amide bonds, see: (a) Kemnitz, C. R.; Loewen, M. J. "Amide Resonance" Correlates with a Breadth of C−N Rotation Barriers. *J. Am. Chem. Soc.* **2007**, *129*, 2521-2528. (b) Glover, S. A.; Rosser, A. A. Reliable Determination of Amidicity in Acyclic Amides and Lactams. *J. Org. Chem.* **2012**, *77*, 5492-5502. (c) Morgan, J.; Greenberg, A.; Liebman, J. F. Paradigms and Paradoxes: O- and N-Protonated Amides, Stabilization Energy and Resonance Energy. *Struct. Chem.* **2012**, *23*, 197-199.

(17) Halima, T.; Zhang, W; Yalaoui, I.; Hong, X.; Yang, Y.; Houk, K.; Newman, S. Palladium-Catalyzed Suzuki−Miyaura Coupling of Aryl Esters. J. Am. Chem. Soc. **2017**, *139*, 1311-1318.

(18) Hirschbeck, V.; Gehrtz, P. H.; Fleischer, I. Metal-Catalyzed Synthesis and Use of Thioesters: Recent Developments. *Chem. Eur. J.* **2018**, *24*, 7092-7107.

(19) (a) Marion, N.; Nolan, S. P. Well-Defined *N*-Heterocyclic Carbenes-Palladium(II) Precatalysts for Cross-Coupling Reactions. *Acc. Chem. Res.* **2008**, *41*, 1440-1449. (b) Li, G.; Lei, P.; Szostak, M.; Casals, E.; Poater, A.; Cavallo, L.; Nolan, S. P. Mechanistic Study of Suzuki-Miyaura Cross-Coupling Reactions of Amides Mediated by [Pd(NHC)(allyl)Cl] Precatalysts. *ChemCatChem* **2018**, *10*, 3096-3106.

(20) Valente, C.; Calimsiz, S.; Hoi, K. H.; Mallik, D.; Sayah, M.; Organ, M. G. The development of bulky palladium NHC complexes for the most-challenging cross-coupling reactions. *Angew. Chem. Int. Ed.* **2012**, *51*, 3314-3332.

(21) Ma, S.; Zhou, T.; Li, G.; Szostak, M. Suzuki-Miyaura Cross-Coupling of Amides using Well-Defined, Air-Stable [$(PR_3)_2Pd(II)X_2$] Precatalysts. *Adv. Synth. Catal.* **2020**, *362*, 1887-1892.

(22) Gildner, P. G.; Colacot, T. J. Reactions of the 21$^{st}$ Century: Two Decades of Innovative Catalyst Design for Palladium-Catalyzed Cross-Couplings. *Organometallics* **2015**, *34*, 5497-5508.

(23) Cox, C.; Lectka, T. Synthetic Catalysis of Amide Isomerization. *Acc. Chem. Res.* **2000**, *33*, 849-858.

(24) Wiberg, K. B. The Interaction of Carbonyl Groups with Substituents. *Acc. Chem. Res.* **1999**, *32*, 922-929.

(25) Chen, M.; Dong, G. Direct catalytic desaturation of lactams enabled by soft enolization. *J. Am. Chem. Soc.* **2017**, *139*, 7757−7760.

(26) Kataoka, K.; Wachi, K.; Jin, X.; Suzuki, K.; Sasano, Y.; Iwabuchi, Y.; Hasegawa, J.; Mizunoa, N.; Yamaguchi, K. CuCl/TMEDA/nor-AZADO-catalyzed aerobic oxidative acylation of amides with alcohols to produce imides. *Chem. Sci.* **2018**, *9*, 4756–4768.

(27) Rahman, M. M.; Buchspies, J.; Szostak, M. *N*-Acylphthalimides: efficient acyl coupling reagents in Suzuki–Miyaura cross-coupling by N–C cleavage catalyzed by Pd–PEPPSI precatalysts. *Catalysts* **2019**, *9*, 129–139.

(28) Chiarotto, I.; Feroci, M.; Orsini, M.; Sotgiu, G.; Inesi, A. Electrogenerated *N*-heterocyclic carbenes: N-functionalization of benzoxazolones. *Tetrahedron* **2009**, *65*, 3704–3710.

(29) Tang, S. -Q.; Bricard, J.; Schmitt, M.; Bihel, F. Fukuyama Cross-Coupling Approach to Isoprekinamycin: Discovery of the Highly Active and Bench-Stable Palladium Precatalyst POxAP. *Org. Lett.* **2019**, *21*, 844−848.

(30) Gobbi, S.; Hu, Q.; Foschi, G.; Catanzaro, E.; Belluti, F.; Rampa, A.; Fimognari, C.; Hartmann, R. W.; Bisi, A. Benzophenones as xanthone-open model CYP11B1 inhibitors potentially useful for promoting wound healing. *Bioorg Chem* **2019**, *86*, 401–409.